Eur. Phys. J. A **12**, 453–477 (2001)

THE EUROPEAN PHYSICAL JOURNAL A

Transport theory for a scalar quark & gluon model

D.S. Isert[a] and S.P. Klevansky

Institut für Theoretische Physik, Philosophenweg 19, D-69120 Heidelberg, Germany

Received: 7 November 2001
Communicated by A. Schäfer

Abstract. A model for scalar quarks and gluons that successfully gives rise to a ln s behavior in high-energy qq scattering and which contains a non-trivial three-gluon vertex is used to study collision theory with the following aspects: i) A three-body interaction simulating QCD is present and ii) particle production and annihilation occur naturally. In this paper, the collision term in the model is examined in detail in the quasiparticle approximation. The construction of cross-sections in which self-energy terms are ordered according to a coupling constant expansion is undertaken. It is shown explicitly which terms of second order are required to obtain the scattering amplitudes that are two body in nature. Additional ordering in the number of colors shows that quark loop diagrams are suppressed and gluon production or scattering processes dominate. It is also shown that a consistent calculation of the scattering graphs at the two-loop level also simultaneously yields terms that renormalize one-loop level graphs. This can then be extended to arbitrary $m \to n$ processes. We examine the constraint equation briefly, discussing the appearance of a width. The issue of pinch singularities is also addressed, and examples of the elimination of such singularities in equilibrium are given explicitly.

PACS. 12.40.-y Other models for strong interactions – 05.20.Dd Kinetic theory – 12.38.Mh Quark-gluon plasma – 24.85.+p Quarks, gluons, and QCD in nuclei and nuclear processes

1 Introduction

Collision theory is now more than a century old, yet over time, as new applications have placed new demands for theoretical exactness in formulation, there remain several unclear points that prohibit direct practical applications. This is unsatisfactory, since a detailed physical understanding of some complex physical phenomena requires a description in terms of non-equilibrium physics. One may think for example of heavy-ion collisions, which simulate conditions in the early universe, and which occurred on an extremely small time scale in which chemical and thermal equilibrium may not both have been reached. An additional degree of complexity is introduced into these modern problems in that phase transitions may occur and these can play an important role.

The fundamentals of collision theory in an empirical formulation were laid down by Boltzmann in 1872 and have since become standard text book material in dealing with non-equilibrium systems [1]. A field-theoretical basis for this so-called transport equation originates from the work of Schwinger [2] and Keldysh [3]. Simultaneously, a constraint equation is shown to be essential for mathematical consistency. From a non-relativistic point of view, the field-theoretical origin of the Boltzmann equation, as a semiclassical equation containing two-body collisions is thus complete. Generalizations of the Boltzmann equation, either relativistically for fermions or bosons, or as a set of fully quantum equations, have been the subject of the last decades. While the exact *formal* equations for the transport and constraint equations have been known for quite some time now, their interpretation in terms of physical functions has been difficult and is only to some extent understood. In relativistic models, it has been shown how two-body collisions arise from the lowest-order terms of the proper self-energy that enters into the transport equation — but here only within a simple model with static interactions. Going beyond this level in an exact fashion within perturbation theory has not been addressed. It is obvious, however, that two-body collisions are insufficient for discussing dense systems, and systems in which three and more body interactions and particle production occur. Here there is a definite need for clarity.

From a technical perspective, the fact that collision theory has developed slowly and continues to develop slowly even after all this time, is that together with the recognition of its possible relevance comes also the undeniable fact that it has a complicated structural basis. A lot of arduous mathematical labor is essential just to establish the basic formal transport and constraint equations.

[a] e-mail: D.Isert@tphys.uni-heidelberg.de

This unfortunately does not lead to a simple and transparent physical picture. Because of this, there are several *ad hoc* approaches which can be commonly found in the literature:

- Many authors rely on an intuitive extrapolation of the semiclassical Boltzmann equation in their applications (see for example, Geiger and Müller [4,5] who examine heavy-ion collisions in extreme conditions). Here an educated guess at an extended Boltzmann equation is made in order to develop a numerical simulation algorithm. In such an approach, often the transport equation alone is examined; the constraint equation is simply neglected. In such studies a first attempt at putting this application on a firm theoretical basis was subsequently made by [6].
- Some authors have centered their investigations on a full quantum treatment of the non-equilibrium Green function equations (see for example [7–9]). This approach has an aesthetic appeal, but in practice, there is little possibility of its application, as the complexity of solving many (16 or more) coupled integro-differential equations can only be performed under severe physical restrictions, namely that of no collisions.

Progress in understanding collision theory has been made with the recent developments in real-time Green function theory to calculate properties of systems in equilibrium. As we have already mentioned, a theoretical methodology for handling non-equilibrium Green functions was developed by Schwinger and Keldysh [2,3]. Later, in the '80s, the development of thermal field theory was initiated by Umezawa [10]. The resulting matrix of real-time Green functions has revealed a striking resemblance to the matrix of Green functions that is obtained in the Schwinger-Keldysh formalism. One can in fact quantifiably demonstrate that Schwinger-Keldysh and thermal field theory yield the same results in the limit that one considers equilibrium systems. The real-time Green function formalism is extremely cumbersome. It is as unwieldy as its non-equilibrium counterpart due to Schwinger and Keldysh. It is especially cumbersome, when contrasted with the elegant formulation of equilibrium field theory by Matsubara, that was developed in the '60s, and which simply makes extensive use of function theory. The historically late development of real-time Green function theory is due to the fact that several difficulties in this approach are immediately evident: Products of retarded and advanced Green functions occur, so that integration along the real axis becomes problematic as the infinitesimal element $\epsilon \to 0$: the contour is pinched and the function is singular. So called pinch singularities also manifest themselves as products of delta functions when working in a causal/acausal framework. The fact now that two completely different formulations of equilibrium field theory exist has enabled one to understand these apparent difficulties in the real-time approach, and this in turn enables one by comparison, to investigate similar situations in the non-equilibrium theory.

In this paper, we do not intend to review all approaches and applications of collision or kinetic theory. Rather our main intention is to investigate certain questions. The first of these is to examine how a perturbative treatment of the collision integral can be expanded to go beyond the standard two-body collisional approach, that in the semiclassical approximation is just the Boltzmann equation. Here the questions in mind are what happens if complex vertices such as three (of four) particle interactions are allowed? What role does particle production play? How can this be systematically incorporated? Furthermore, since we are intrinsically interested in a theory of quarks and gluons, we wish to answer these questions without raising further difficulties like do our approximations preserve gauge invariance? Thus, in order to concentrate on the development of the collision integral, we choose a field theory of quarks and gluons which is simplistic: both degrees of freedom are chosen to be scalar. In addition, a three-body self-interacting gluon vertex is introduced. In this form, the model becomes interesting from another point of view. This scalar quark and gluon model is one of the predecessors of QCD in describing S-matrix behavior and leads to the existence of pomerons. Thus this theory produces the correct $\log s$ behavior in the calculations of elastic quark-quark scattering at high energies. The origin of this behavior is explicitly evident; it arises as a consequence of a specific sum of leading terms, *viz* ladder diagrams. Consequently another question dealt with in this study is to examine whether the ladder sum appears as a natural approximation in the collision integral when multiple gluons are produced. Our interest in connecting the pomeron picture with a quark and gluon picture lies also in the application of pomeron phenomenology to high-energy collisions. The VENUS-model of heavy-ion collisions for example, is based on pomeron exchange. The application of this model has been most successful in the past (see, *e.g.*, ref. [11]), but is inadequate for describing very energetic collisions such as are expected at the LHC. With this in mind, a natural step is to ask the question as to whether a simple link can be made from a quark and gluon model to pomeron behavior from a non-equilibrium starting point, given the fact that the original theory is known to lead to the correct scattering at high energies. Although pomeron behavior can be directly deduced from QCD per se, we use this toy model here for its analytic simplicity. We do not regard it as a substitute for QCD, and believe that the next real steps in regarding QCD proper must be undertaken. To our knowledge, there is no detailed study of this model in equilibrium; and we do not undertake this here.

For completeness, in addition to the papers on non-equilibrium theory already cited, we draw attention in general to the work of other authors in non-equilibrium theory such as ref. [12] in which the formalistic consistency required by the constraint approach was first emphasized, ref. [13], who insert dynamical spectral functions into a semi-classical approximation, the classical approach of ref. [14], and lastly the field-theoretical approach of ref. [15] for scalar electrodynamics and long wavelength color fluctuations in QCD. This last reference contains a wealth of further references.

This paper is structured as follows. In the following section, we briefly review the model of scalar quarks and gluons, and indicate the results for elastic quark-quark scattering. In sect. 3, for notational clarity, we then write down the basic equations required for transport theory for our scalar model in the Schwinger-Keldysh approach. We first assume the quasiparticle approximation is valid, and investigate the collision integral of the transport equation in detail, identifying scattering graphs, particle renormalization graphs and graphs which appear to be singular. These issues, together with the mean-field approximation, are discussed in sects. 4-7. In sect. 8, we return to the constraint equation, and examine the consequences of assuming a finite width. We summarize and conclude in sect. 9. Four appendices are attached: in A, we summarize real-time field theory, while B contains some information on the non-equilibrium formulation. In appendix C, technical color sums are listed, and appendix D gives an example of the cancellation of pinch singularities for our model in equilibrium.

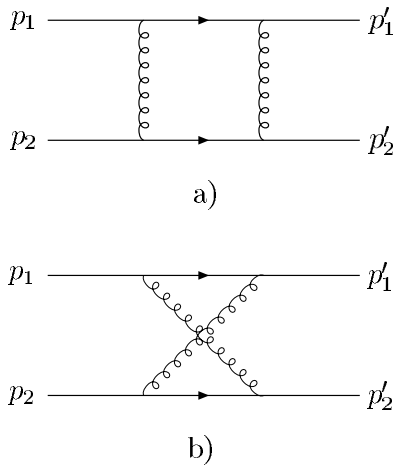

Fig. 1. Leading-order contribution to pomeron exchange for elastic quark-quark scattering.

2 Model of scalar quarks and gluons

In this section, we introduce and discuss the scalar partonic model, and give the equations of motion for quark and gluon fields. We briefly review high-energy scattering within this model.

2.1 Scalar partonic model

We study a partonic model of QCD inspired by Polkinghorne [16] and used by Forshow and Ross [17] that contains scalar partons. Quarks and antiquarks are described by complex scalar fields ϕ, and gluons as the scalar field χ coupled through the Lagrangian

$$\mathcal{L}=\partial^\mu\phi^{\dagger i,l}\partial_\mu\phi_{i,l}+\frac{1}{2}\partial^\mu\chi_{a,r}\partial_\mu\chi^{a,r}-\frac{m^2}{2}\chi_{a,r}\chi^{a,r}$$
$$-gm\phi^{\dagger i,l}(T^a)^j_i(T^r)^m_l\phi_{j,m}\chi_{a,r}-\frac{gm}{3!}f_{abc}f_{rst}\chi^{a,r}\chi^{b,s}\chi^{c,t}. \tag{1}$$

The quark fields are regarded as massless, as one generally assumes for high-energy processes, while the gluons are usually assigned a mass m *a priori* in order to avoid infra-red divergences. There is an interaction between quarks and gluons as well as a cubic self-interaction between gluons. Since in QCD the quartic interaction between gluons leads inelastic qq scattering to terms which are sub-leading in ln s, such a quartic interaction among gluons is not included within this model.

One notes that both the quark and gluon fields carry two labels. Both labels refer to color groups. The fact that a direct product of two color groups is necessary can be seen on examining the three-gluon vertex term. This term must be symmetric under the exchange of two gluons since they are bosons. In addition, one expects that the interaction vertex should be proportional to the (antisymmetric) structure constants of the color group. A single color group cannot meet these requirements, and the simplest combination which can is a product of two $SU(N_c)$ groups. Thus the gluon field carries two color indices $(a, r = 1...(N_c^2-1))$. Since the quark field transforms in the fundamental representation of both of these $SU(N_c)$ groups, it must carry two color indices as well $(i, l = 1...N_c)$. The matrices T^a and T^r are the generators and f_{abc} and f_{rst} are the structure constants for the two $SU(N_c)$ groups, respectively. Thus they satisfy

$$[T^a,T^b]=if_{abc}T^c, \qquad [T^r,T^s]=if_{rst}T^t. \tag{2}$$

Note in eq. (1) that the flavor index of the quark fields is suppressed.

The equations of motion for the fields can be derived from the Euler-Lagrange equations. They are

$$\Box\phi^{(\dagger)i,l}=-gm(T^a)^i_j(T^r)^l_m\phi^{(\dagger)j,m}\chi_{a,r} \tag{3}$$

for the (anti-)quarks and

$$(\Box+m^2)\chi^{a,r}=-gm[\phi^{\dagger i,l}(T^a)^i_j(T^r)^m_l\phi_{j,m}$$
$$+f^{abc}f^{rst}\chi_{b,s}\chi_{c,t}] \tag{4}$$

for the gluons.

2.2 Elastic qq scattering at high energies

The main advantage of this simple partonic model is that a calculation of the elastic quark-quark scattering amplitude at high energies at $T = 0$ reflects pomeron behavior. In this section, we simply quote these results, and for details, we refer the reader to [17]. Note that these calculations are performed in equilibrium and at $T = 0$ in contrast to the rest of this paper.

Quark-quark scattering is calculated via the exchange of a color singlet. It is assumed that the two quarks emerge from the scattering with the same color with which they entered and that they have different flavors. Therefore, one has to consider only diagrams with at least two exchanged gluons, and one can neglect diagrams with quarks that are exchanged in the t-channel. The incoming quarks have momenta p_1 and p_2, respectively. To lowest order, this process is shown in fig. 1. Denoting the transferred momentum as $q = p_1 - p_2$, the Mandelstam variables read as $s = (p_1 + p_2)^2$ and $t = q^2$. In the case of fig. 1, it is easy to show that fig. 1b) follows from fig. 1a) only by a kinematical transformation, so that it is only necessary to calculate graphs of type (a). The imaginary part of the amplitude can be immediately identified to be

$$\Im\mathcal{A} = \frac{1}{2}\int \mathrm{d}(\mathrm{PS}^2)\, \mathcal{A}_0^{(g)}(k)\, \mathcal{A}_0^{(g)\dagger}(k-g), \tag{5}$$

where $\mathcal{A}_0^{(g)}(k) = -g^2 m^2\, 1/(k^2 - m^2)$, and $\int \mathrm{d}(\mathrm{PS}^2)$ refers to the phase space of the two lines which are cut in the Sudakov fashion, *i.e.*

$$\int \mathrm{d}(\mathrm{PS}^2) = \int \frac{\mathrm{d}^4 l}{(2\pi)^3}\frac{\mathrm{d}^4 l'}{(2\pi)^3}\delta(l^2)\delta(l'^2)(2\pi)^4 \times\delta^4(p_1 + p_2 - l - l'). \tag{6}$$

One integral can be immediately performed, leaving one further integral in one variable, which is denoted as k. The further calculations are now performed in the Regge limit, $s \gg |t|$. Therefore it is useful to parametrize the integrated momenta in terms of Sudakov parameters ρ and λ:

$$k = \rho p_1 + \lambda p_2 + k_\perp, \tag{7}$$

where $k_\perp$ is the momentum transverse to p_1 and p_2 and this two-dimensional vector is represented by the boldface $\mathbf{k}$. In identifying further graphs which give rise to contributions $\Im\mathcal{A}(s,t) \propto s^{\alpha(t)}$, one arrives at the set with n-rungs $n = 1, .., \infty$, as is indicated in fig. 2. The dashed line indicates the cut taken for the direct application of the Cutkosky rules. Applying these rules and keeping only the leading $\ln s$ contributions in evaluating the infinite sum of uncrossed ladder diagrams, one obtains the following result for the imaginary part of the scattering amplitude

$$\Im\mathcal{A}(s,t) = \frac{(N_c^2-1)^2}{16N_c^4}\frac{g^4 m^4}{16\pi^2 s} \times \int \mathrm{d}^2\mathbf{k}\, \frac{1}{(\mathbf{k}^2+m^2)((\mathbf{k}-\mathbf{q})^2+m^2)} \left(\frac{s}{|t|}\right)^{1+\alpha_P(t)}, \tag{8}$$

with the trajectory

$$\alpha_P(t) \approx -1 + \frac{g^2 N_c^2}{16\pi^2}\left(1 + \frac{t}{6m^2}\right). \tag{9}$$

In the Regge limit, the real part of $\mathcal{A}(s,t)$ vanishes. Therefore $\mathcal{A}(s,t)$ is purely imaginary and given by eq. (8).

We point out that the selection of ladder diagrams for the evaluation of the scattering amplitude, as indicated in fig. 2 is highly suggestive, particularly with the cut drawn in. One might wish to conclude that a) gluon production is dominant, and b) that only ladder type graphs need be considered in constructing gluon emission/absorptive processes. As will be seen in transport theory, however, one finds that a) is true, having its basis in the $1/N_c$ expansion, but b) cannot be justified, as it depends on the special kinematical assumptions that are applicable to the quark-quark scattering amplitude, but which do not occur in the self-energy evaluation.

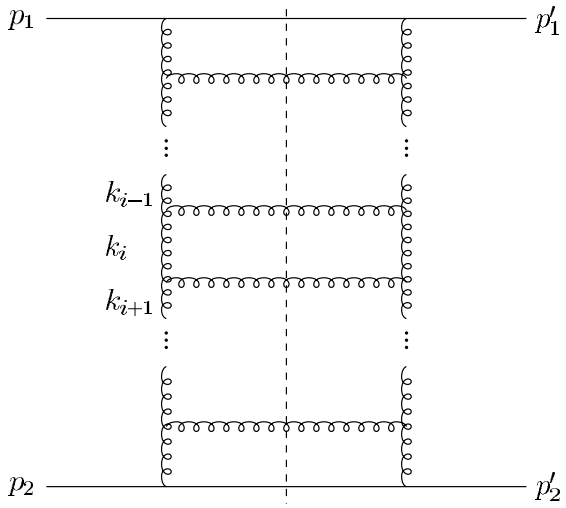

Fig. 2. n-rung ladder diagram with cut line (dashed line).

3 Transport theory for interacting bosonic fields

In this section, we briefly introduce the Schwinger-Keldysh formalism and the quasiparticle approximation. A comparison with the equilibrium real-time formulation of finite-temperature field theory is made in appendix A.

For the purpose of establishing our notation, we give the basic definitions and refer the reader to standard texts [18–20]. The quark Green functions in the Schwinger-Keldysh formalism [2,3] are defined as

$$\begin{aligned}
iS^c(x,y) &= \left\langle T\phi^{i,l}(x)\phi^{\dagger j,m}(y)\right\rangle \\
&\quad - \left\langle \phi^{i,l}(x)\right\rangle\left\langle \phi^{\dagger j,m}(y)\right\rangle = iS^{--}(x,y)\,, \\
iS^a(x,y) &= \left\langle \tilde{T}\phi^{i,l}(x)\phi^{\dagger j,m}(y)\right\rangle \\
&\quad - \left\langle \phi^{i,l}(x)\right\rangle\left\langle \phi^{\dagger j,m}(y)\right\rangle = iS^{++}(x,y)\,, \\
iS^>(x,y) &= \left\langle \phi^{i,l}(x)\phi^{\dagger j,m}(y)\right\rangle \\
&\quad - \left\langle \phi^{i,l}(x)\right\rangle\left\langle \phi^{\dagger j,m}(y)\right\rangle = iS^{+-}(x,y)\,, \\
iS^<(x,y) &= \left\langle \phi^{\dagger j,m}(y)\phi^{i,l}(x)\right\rangle \\
&\quad - \left\langle \phi^{i,l}(x)\right\rangle\left\langle \phi^{\dagger j,m}(y)\right\rangle = iS^{-+}(x,y)\,,
\end{aligned} \tag{10}$$

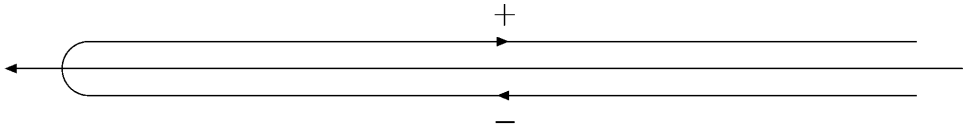

Fig. 3. Closed time path.

and for the gluons as

$$\begin{aligned}
iG^c(x,y) &= \left\langle T\chi^{a,r}(x)\chi^{b,s}(y)\right\rangle \\
&\quad - \left\langle\chi^{a,r}(x)\right\rangle\left\langle\chi^{b,s}(y)\right\rangle = iG^{--}(x,y)\,, \\
iG^a(x,y) &= \left\langle \tilde{T}\chi^{a,r}(x)\chi^{b,s}(y)\right\rangle \\
&\quad - \left\langle\chi^{a,r}(x)\right\rangle\left\langle\chi^{b,s}(y)\right\rangle = iG^{++}(x,y)\,, \\
iG^{>}(x,y) &= \left\langle\chi^{a,r}(x)\chi^{b,s}(y)\right\rangle \\
&\quad - \left\langle\chi^{a,r}(x)\right\rangle\left\langle\chi^{b,s}(y)\right\rangle = iG^{+-}(x,y)\,, \\
iG^{<}(x,y) &= \left\langle\chi^{b,s}(y)\chi^{a,r}(x)\right\rangle \\
&\quad - \left\langle\chi^{a,r}(x)\right\rangle\left\langle\chi^{b,s}(y)\right\rangle = iG^{-+}(x,y)\,. \qquad (11)
\end{aligned}$$

Here T and $\tilde{T}$ are the usual time and anti-time ordering operators, respectively. As given, the Green functions fall along the contour designated in fig. 3. Our convention follows that of ref. [20]. They satisfy a Dyson equation that introduces the matrix of self-energies for either the quark or gluonic sectors, $\underline{\Sigma}_q$ or $\underline{\Sigma}_g$. Using a generic notation, $\underline{D} = \underline{S}$ or $\underline{G}$ and $\underline{\Pi} = \underline{\Sigma}_q$ or $\underline{\Sigma}_g$ as appropriate, one may write

$$\begin{aligned}
\underline{D}(x,y) &= \underline{D}^0(x,y) - \int \mathrm{d}^4z\mathrm{d}^4w\,\underline{D}^0(x,w)\underline{\Pi}(w,z)\underline{D}(z,y) \\
&= \underline{D}^0(x,y) - \int \mathrm{d}^4z\mathrm{d}^4w\,\underline{D}(x,w)\underline{\Pi}(w,z)\underline{D}^0(z,y). \qquad (12)
\end{aligned}$$

In a standard fashion, the transport and constraint equations can be derived, and this is summarized briefly in appendix B. In terms of the center-of-mass variable $X = (x+y)/2$ and the Fourier transform variable p conjugate to the relative distance $u = x - y$, or Wigner transform, the equations that one obtains for the off diagonal Green functions, corresponding to the transport and constraint equations are

$$-2ip\partial_X D^{-+}(X,p) = I_-\,, \qquad \text{transport} \qquad (13)$$

and

$$\left(\frac{1}{2}\Box_X - 2p^2 + 2M^2\right) D^{-+}(X,p) = I_+, \qquad \text{constraint}\,, \qquad (14)$$

respectively, where M is a generic parton mass, $M = m$ for the gluons and $M = 0$ for the quarks. $I_\mp$ is an abbreviation for the combined functions

$$I_\mp = I_{\rm coll} + I^{\rm A}_\mp + I^{\rm R}_\mp, \qquad (15)$$

and $I_{\rm coll}$ is the collision term,

$$\begin{aligned}
I_{\rm coll} &= \Pi^{-+}(X,p)\hat{\Lambda}D^{+-}(X,p) \\
&\quad - \Pi^{+-}(X,p)\hat{\Lambda}D^{-+}(X,p) = I^{\rm gain}_{\rm coll} - I^{\rm loss}_{\rm coll}. \qquad (16)
\end{aligned}$$

$I^{\rm R}_\mp$ and $I^{\rm A}_\mp$ are terms containing retarded and advanced components, respectively

$$I^{\rm R}_\mp = -\Pi^{-+}(X,p)\hat{\Lambda}D^{\rm R}(X,p) \pm D^{\rm R}(X,p)\hat{\Lambda}\Pi^{-+}(X,p) \qquad (17)$$

and

$$I^{\rm A}_\mp = \Pi^{\rm A}(X,p)\hat{\Lambda}D^{-+}(X,p) \mp D^{-+}(X,p)\hat{\Lambda}\Pi^{\rm A}(X,p). \qquad (18)$$

In eqs. (16) to (18), the operator $\hat{\Lambda}$ is given by

$$\hat{\Lambda} := \exp\left\{\frac{-i}{2}\left(\overleftarrow{\partial}_X\overrightarrow{\partial}_p - \overleftarrow{\partial}_p\overrightarrow{\partial}_X\right)\right\}. \qquad (19)$$

In order to proceed further, we have to calculate the self-energies Π that occur in eqs. (16) to (18). The simplest possible approximation is the so-called quasiparticle approximation, in which a *free* scalar parton of mass M is assigned the Green functions

$$\begin{aligned}
iD^{-+}(X,p) &= \frac{\pi}{E_p}\{\delta(E_p - p^0)f_a(X,p) \\
&\quad + \delta(E_p + p^0)\bar{f}_{\bar{a}}(X,-p)\}\,, \qquad (20) \\
iD^{+-}(X,p) &= \frac{\pi}{E_p}\{\delta(E_p - p^0)\bar{f}_a(X,p) \\
&\quad + \delta(E_p + p^0)f_{\bar{a}}(X,-p)\}\,, \qquad (21) \\
iD^{--}(X,p) &= \frac{i}{p^2 - M^2 + i\epsilon} + \Theta(-p^0)iD^{+-}(X,p) \\
&\quad + \Theta(p^0)iD^{-+}(X,p) \\
&= \frac{i}{p^2 - M^2 + i\epsilon} + \frac{\pi}{E_p}\{\delta(E_p - p^0)f_a(X,p) \\
&\quad + \delta(E_p + p^0)f_{\bar{a}}(X,-p)\}\,, \qquad (22) \\
iD^{++}(X,p) &= \frac{-i}{p^2 - M^2 - i\epsilon} + \Theta(-p^0)iD^{+-}(X,p) \\
&\quad + \Theta(p^0)iD^{-+}(X,p) \\
&= \frac{-i}{p^2 - M^2 - i\epsilon} + \frac{\pi}{E_p}\{\delta(E_p - p^0)f_a(X,p) \\
&\quad + \delta(E_p + p^0)f_{\bar{a}}(X,-p)\}\,, \qquad (23)
\end{aligned}$$

with $E_p^2 = p^2 + M^2$, and which are given in terms of the corresponding scalar quark and gluon distribution functions, $f_a(X,p)$, and $\bar{f}_a = 1 + f_a$, where a denotes the parton type $a = q, g$.

Our task in this paper is to construct an equation for the distribution functions for quarks and gluons $f_a(X,p)$ from eqs. (13) to (18), using the quasiparticle Green functions of the form given in eqs. (20) to (23). To do so, it is necessary to integrate the entire eq. (13) and eq. (14) over an interval $\Delta_\pm$ which contains $\pm E_p(X)$. To lowest order

in an expansion that sets $\hat{\Lambda} = 1$, the terms $I_{\pm}^{\mathrm{R,A}}$ simplify considerably. In particular

$$I_{-}^{\mathrm{R,A}} = 0 \tag{24}$$

so that I_{-} in eqs. (13) and (15) becomes

$$I_{-} = I_{\mathrm{coll}}. \tag{25}$$

The integration of eq. (13) over $\Delta_{\pm}$ requires a construction of the form

$$J_{\mathrm{coll}} = J_{\mathrm{coll}}^{\mathrm{gain}} - J_{\mathrm{coll}}^{\mathrm{loss}} = \int_{\Delta^+} \mathrm{d}p_0\, I_{\mathrm{coll}}^{\mathrm{gain}} - \int_{\Delta^+} \mathrm{d}p_0\, I_{\mathrm{coll}}^{\mathrm{loss}} \tag{26}$$

for the right-hand side. This integral can be easily performed, and one has

$$\begin{aligned} J_{\mathrm{coll}} &= \int_{\Delta^+} \mathrm{d}p_0\, \Pi^{-+}(X,p)\, D^{+-}(X,p) \\ &\quad - \int_{\Delta^+} \mathrm{d}p_0\, \Pi^{+-}(X,p)\, D^{-+}(X,p) \\ &= -i\frac{\pi}{E_p}\, \Pi^{-+}(X, p_0 = E_p, \vec{p})\, \bar{f}_a(X,\vec{p}) \\ &\quad + i\frac{\pi}{E_p}\, \Pi^{+-}(X, p_0 = E_p, \vec{p})\, f_a(X,\vec{p}), \end{aligned} \tag{27}$$

i.e. the off-diagonal quasiparticle self-energies are required to be calculated on-shell.

Therefore the complete transport equation reads

$$\begin{aligned} 2p\partial_X f_a(X,\vec{p}) &= i\Pi^{-+}(X, p_0 = E_p, \vec{p})\, \bar{f}_a(X,\vec{p}) \\ &\quad - i\Pi^{+-}(X, p_0 = E_p, \vec{p})\, f_a(X,\vec{p}). \end{aligned} \tag{28}$$

In the same approximation, *i.e.* setting $\hat{\Lambda} = 1$ and neglecting the term proportional to $\Box_X$, the constraint equation takes the form

$$\begin{aligned} &\left[-2p^2 + 2M^2 - 2\Pi^{\mathrm{A}}(X,p)\right] D^{-+}(X,p) = \\ &\Pi^{-+}(X,p)\, D^{+-}(X,p) - \Pi^{+-}(X,p)\, D^{-+}(X,p) \\ &\quad -2\Pi^{-+}(X,p)\, D^{\mathrm{R}}(X,p). \end{aligned} \tag{29}$$

In case of vanishing self-energies, eq. (28) is the equation for free streaming,

$$2p\partial_X f_a(X,\vec{p}) = 0, \tag{30}$$

while the constraint equation (29) becomes after an integration over Δ_+ :

$$(E_p^2 - \vec{p}^{\,2} - M^2) f_a(X,\vec{p}) = 0. \tag{31}$$

The last equation is the expression of the fact that the partons have to be on mass-shell, and is consistent with the quasiparticle assumption, eqs. (20) to (23) made in the first place.

Let us now examine the transport equation further. Since the number of particles can only be changed via collisions, the right-hand side of eq. (28) is called the collision term. The second term of the right-hand side is proportional to f_a and is therefore identified as the loss term [21], while the first one, proportional to $\bar{f}_a = 1 + f_a$, is identified as a gain term. Naturally, one would expect that it should always be possible to express the collision term in terms of differential scattering cross-sections as occurs in the Boltzmann equation when only two-body processes are present, or alternatively in terms of transition matrix elements.

Several authors have followed this line of thought: for some simple scalar models [22] and the NJL model [9], which contain only a simple form of interaction, it has been shown rigorously that the theoretical generalization of the non-relativistic formalism indeed leads to the relativistic Boltzmann equation with two-body scattering. Particularly within QCD and quark-gluon dynamics, however this generalization is far more difficult. Reference [6] also attempts a formal identification of the Boltzmann equation from quark-gluon dynamics to the two-body scattering level in the Keldysh formalism. This derivation is however in itself at the two-body level theoretically incomplete. Furthermore, the two-body level is insufficient for the description of the complex type of processes that can occur in such systems, such as multiple gluon production. A precise theoretical understanding of how such a transport theory should be generalized to include particle production within a non-Abelian model has not been addressed. Rather, *ad hoc* assumptions for the form of such a generalized collision term have been made on the basis of empirical expectations (see for example [4]).

Our task is therefore to investigate the collision term in a non-Abelian theory exactly in the two-body level and beyond this, and to express, if possible, the self-energies in terms of cross-sections or, equivalently, in terms of scattering amplitudes. Due to our particular choice of masses (quarks massless, gluons massive) the lowest-order processes that can occur, are the annihilation process $q\bar{q} \to g$ and the decay process $g \to q\bar{q}$. One expects to obtain these processes from the mean-field self-energies. Two-loop self-energies, on the other hand, should yield $2 \to 2$ scattering processes. These processes, which are far more complex than in a simple model with a static interaction as in [9] for example, are detailed here. This complexity also occurs in the QCD case, and the results here can easily be extrapolated to this, in order to complete the derivations attempted in [6]. We then examine higher-order contributions to the aforementioned processes.

To render the calculations tractable we will neglect the constraint equation (14) beyond the Hartree level in the following sections. Its influence will be discussed in sect. 8.

4 The collision integral — mean-field self-energies

In this section, we return to the transport equation eq. (28). We evaluate the self-energies to first order in the interaction strength and illustrate their role in the transport equation in the semi-classical limit.

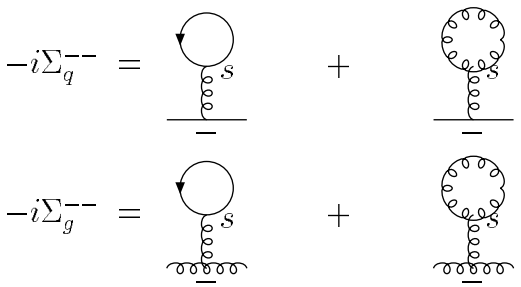

Fig. 4. Quark and gluon generic Hartree self-energies. Solid lines refer to quarks, wavy lines to gluons.

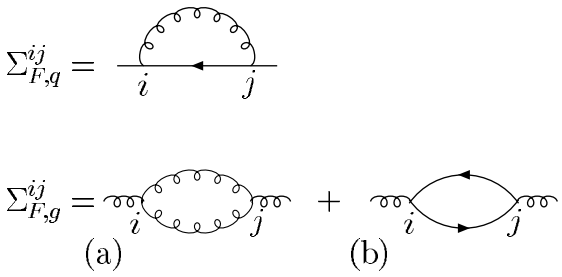

Fig. 5. Quark and gluon generic one-loop self-energies. The quark self-energy plus the first gluon self-energy are Fock diagrams, while (b) is a polarization insertion.

4.1 Hartree self-energies

For the scalar parton model, two generic kinds of Hartree graphs can be identified in the quark and gluon self-energies. These are depicted in fig. 4. For Hartree diagrams of any kind, off diagonal self-energies are per definition zero and only diagonal elements can possibly be constructed, *i.e.* Σ_H^{--} or Σ_H^{++}. However, all such diagrams vanish identically in this model. The reason for this lies in the color factors: for the quark self-energy graph in fig. 4 that contains a quark-loop, a single $SU(3)$ color group leads to the associated color factor

$$F_{H,q} = t^a_{ii}\mathrm{tr}(t^a) = 0, \tag{32}$$

since $t_a = \lambda^a/2$, where λ^a are the Gell-Mann matrices. In the above expression, i denotes the external quark momentum and is therefore not to be summed over. For the quark self-energy containing a gluon line, the color factor for a single $SU(3)$ group is also vanishing,

$$F_{H,g} = t^a_{ii}T^a_{bb} = -it^a_{ii}f_{abb} = 0. \tag{33}$$

Similar arguments apply to the gluon self-energies. Thus, no mass renormalization occurs due to Hartree terms.

A semiclassical expansion of the transport and constraint equations thus leads to free streaming described by eqs. (30) and (31).

4.2 Fock self-energies

The next type of graph contributing to the mean-field expansion is the Fock term. The generic diagrams for the quark and gluon self-energies are shown in fig. 5. (Figure 5(b) is strictly speaking a vacuum polarization graph for the gluons.)

We start with the quark sector and examine as an example, the gain term generated by the Fock term $\Sigma^{-+}_{F,q}(X,p)$. By inspection, one has

$$i\Sigma^{-+}_{F,q}(X,p) = -g^2m^2F^2_{F,q}\int\frac{\mathrm{d}^4p_1}{(2\pi)^4}\int\frac{\mathrm{d}^4p_2}{(2\pi)^4} \times S^{-+}(X,p_1)G^{+-}(X,p_2)(2\pi)^4\delta^{(4)}(p-p_1+p_2), \tag{34}$$

and $F_{F,q}$ is the Fock color factor for a single $SU(N_c)$ group,

$$F_{F,q} = t^a_{ij}t^a_{ji} = \frac{N_c^2-1}{2N_c}\delta_{ii}. \tag{35}$$

The contribution to the collision term that this makes, using eq. (27) is

$$J^{\mathrm{gain}}_{F,\mathrm{coll}} = -i\frac{\pi}{E_p}\Sigma^{-+}_{F,q}(X,p_0=E_p,\vec{p})\bar{f}_q(X,\vec{p}), \tag{36}$$

which, on inserting the explicit expressions for $S^{-+}(X,p)$ and $G^{+-}(X,p)$ from eqs. (20) and (21) leads to four distinct terms,

$$J^{\mathrm{gain}}_{F,\mathrm{coll}} = -g^2m^2F_F^2\frac{\pi}{E_p}\int\frac{\mathrm{d}^4p_1}{(2\pi)^4}\int\frac{\mathrm{d}^4p_2}{(2\pi)^4} \times(2\pi)^4\delta^{(4)}(p+p_1-p_2)\frac{\pi}{E_1}\frac{\pi}{E_2}\sum_{i=1}^{4}T_i, \tag{37}$$

where

$$\begin{aligned}
T_1 &= \delta(E_1-p_1^0)\delta(E_2-p_2^0)\bar{f}_{\bar{q}}(X,p_1)f_g(X,p_2)\bar{f}_q(X,\vec{p}),\\
T_2 &= \delta(E_1-p_1^0)\delta(E_2+p_2^0)\bar{f}_{\bar{q}}(X,p_1)\bar{f}_g(X,-p_2)\bar{f}_q(X,\vec{p}),\\
T_3 &= \delta(E_1+p_1^0)\delta(E_2+p_2^0)f_q(X,-p_1)\bar{f}_g(X,-p_2)\bar{f}_q(X,\vec{p}),\\
T_4 &= \delta(E_1+p_1^0)\delta(E_2-p_2^0)f_q(X,-p_1)f_g(X,p_2)\bar{f}_q(X,\vec{p}).
\end{aligned} \tag{38}$$

By attributing unbarred functions f to incoming particles and barred functions $\bar{f}$ to outgoing ones, one can see that $T_1..T_4$ correspond to the processes $g\to q\bar{q}$, $\emptyset\to q\bar{q}g$, $q\to qg$ and $qg\to q$. The last three of these are kinematically forbidden, while the former is possible, since the gluons are endowed with a finite mass. Performing the integrals over p_1^0 and p_2^0, eq. (37) becomes

$$J^{\mathrm{gain}}_{F,\mathrm{coll}} = -\frac{\pi}{E_p}\int\frac{\mathrm{d}^3p_1}{(2\pi)^32E_1}\frac{\mathrm{d}^3p_2}{(2\pi)^32E_2}(2\pi)^4\delta^{(4)}(p+p_1-p_2) \times|\mathcal{M}_{g\to q\bar{q}}|^2f_g(X,\vec{p}_2)\bar{f}_{\bar{q}}(X,\vec{p}_1)\bar{f}_q(X,\vec{p}). \tag{39}$$

The loss term is obtained in a similar fashion or by exchanging f with $\bar{f}$, since the matrix element is symmetric. Combining both terms, the revised transport equation for quarks is obtained from eq. (28) as

$$\begin{aligned}
2p\partial_X f_q(X,\vec{p}) = \int&\frac{\mathrm{d}^3p_1}{(2\pi)^32E_1}\frac{\mathrm{d}^3p_2}{(2\pi)^32E_2}\\
&\times(2\pi)^4\delta^{(4)}(p+p_1-p_2)|\mathcal{M}_{g\to q\bar{q}}|^2\\
&\times\left[f_g(X,\vec{p}_2)\bar{f}_{\bar{q}}(X,\vec{p}_1)\bar{f}_q(X,\vec{p})\right.\\
&\left.-\bar{f}_g(X,\vec{p}_2)f_{\bar{q}}(X,\vec{p}_1)f_q(X,\vec{p})\right].
\end{aligned} \tag{40}$$

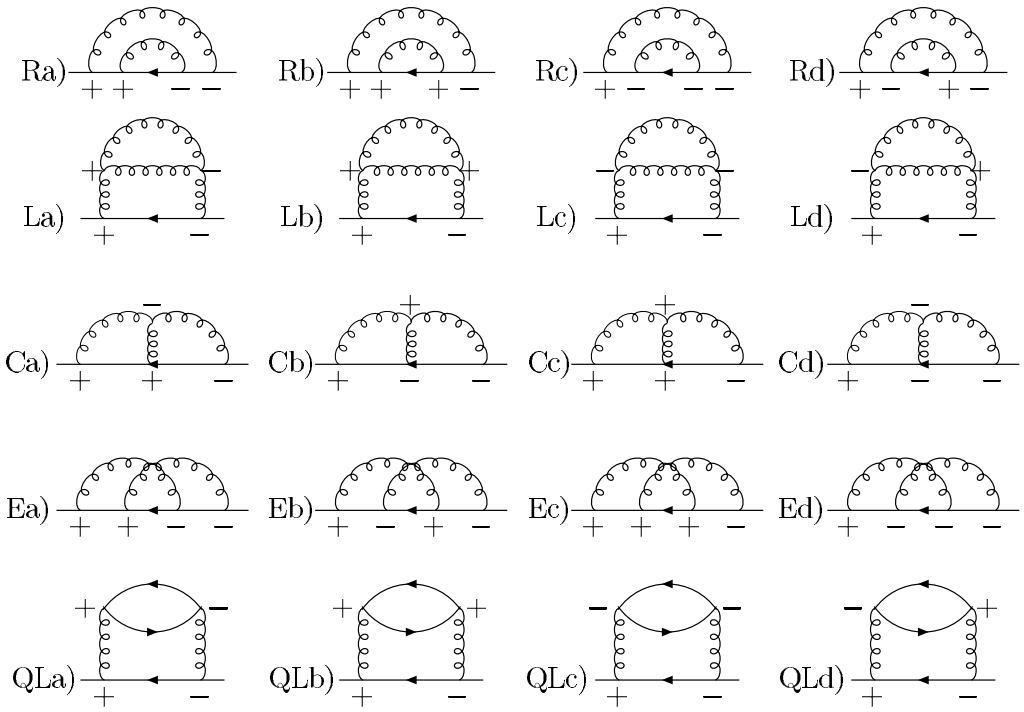

Fig. 6. All diagrams contributing to $\Sigma^{(2)+-}$.

This is the final expression for the Fock transport equation. One can alternatively introduce a cosmetic recombination or decay rate in which case eq. (40) can be written symbolically as

$$2p\partial_X f_q(X,\vec{p}) = \int \frac{\mathrm{d}^3p_1}{(2\pi)^3 2E_1} \int \mathrm{d}\Omega \frac{\mathrm{d}\sigma}{\mathrm{d}\Omega}\bigg|_{q\bar{q}\to g} F \times \left[f_g(X,\vec{p}_2)\bar{f}_{\bar{q}}(X,\vec{p}_1)\bar{f}_q(X,\vec{p}) - \bar{f}_g(X,\vec{p}_2)f_{\bar{q}}(X,\vec{p}_1)f_q(X,\vec{p})\right], \quad (41)$$

where F is the flux factor, and

$$\int \mathrm{d}\Omega \frac{\mathrm{d}\sigma}{\mathrm{d}\Omega} = \int \mathrm{d}Q \frac{|\mathcal{M}|^2}{F} \quad (42)$$

with the invariant phase space factor $\mathrm{d}Q$ given as $\mathrm{d}Q = (2\pi)^4\delta^{(4)}(p+p_1-p_2)\,\mathrm{d}^3p_2/((2\pi)^3 2E_2)$.

An analysis of the self-energy graph 5(a) of the gluon sector, $\Sigma^{-+}_{F,g(a)}(X,p)$ along the previous lines leads to processes $g \to gg$, $\emptyset\to ggg$, and $gg \to g$, all of which are kinematically prohibited. One thus obtains

$$(J^{\mathrm{coll}(a)}_{F,\mathrm{gain/loss}})_{\mathrm{gluonic\ graph}} = 0. \quad (43)$$

This can be attributed to the fact that the self-energies are evaluated on-shell, *i.e.* we may write

$$\Sigma^{-+}_{F,g(a)}(X,p_0=E_p,\vec{p}) = \Sigma^{+-}_{F,g(a)}(X,p_0=E_p,\vec{p}) = 0, \quad (44)$$

which is the statement that an on-shell particle cannot decay into two on-shell particles of the same kind.

The second graph in the gluonic case does not vanish. This self-energy $\Sigma^{-+}_{F,g(b)}$ that enters into the description of the gain in gluons, is precisely that given in eq. (34), but with $G^{+-}(X,p_2)$ replaced by $S^{+-}(X,p_2)$. The color factor in this case is also modified, being $F_{F,g} = 1/2\delta^{aa}$. An analysis of the self-energy along the same lines leads to the processes $q \to qg$, $\bar{q} \to \bar{q}g$, $\emptyset\to gq\bar{q}$ and $q\bar{q} \to g$, the last of which is the only term that can contribute. Thus the time evolution of the gluon distribution function is given by

$$2p\partial_X f_g(X,\vec{p}) = \int \frac{\mathrm{d}^3p_1}{(2\pi)^3 2E_1}\frac{\mathrm{d}^3p_2}{(2\pi)^3 2E_2} \times(2\pi)^4\delta^{(4)}(p+p_1-p_2)|\mathcal{M}_{g\to q\bar{q}}|^2 \times \left[f_q(X,\vec{p}_2)f_{\bar{q}}(X,\vec{p}_1)\bar{f}_g(X,\vec{p}) - \bar{f}_q(X,\vec{p}_2)\bar{f}_{\bar{q}}(X,\vec{p}_1)f_g(X,\vec{p})\right]. \quad (45)$$

We conclude this section by commenting the result that while the Fock term 5(a) for gluons vanishes identically, the Fock term for the quark self-energy does not. A term of this kind occurs in this model because the quarks are massless, while the gluons are massive. The relevance of this Fock term thus depends on the form of the underlying theory.

5 The collision integral — beyond the mean field

For clarity, we will consider in the following only the quark sector in detail. The calculations for the gluonic sector are similar. To proceed further in calculating the collision integral of eq. (27) to next to leading order, we require the off-diagonal self-energy with two loops. To be specific, let

us consider first the loss term for which we need $\Sigma^{(2)+-}$. All of its two-loop contributions are shown in fig. 6. According to their topology, we denote these graphs as rainbow (R), ladder (L), cloud (C), exchange (E) and quark loop graphs (QL). In addition to this, one has to sum over the inner vertices. There are four possibilities of arranging the signs at the inner vertices, which yields the diagrams a) to d) for every type of topology.

5.1 2 → 2 scattering processes

Let us deal first with the diagrams R a), L a), C a), C b), E a), E b) and QL a) of fig. 6. All of these diagrams are necessary to obtain all possible $2 \to 2$ scattering processes as we will now show.

We first note that the diagram E b) is the exchange graph of QL a), because both of these diagrams contain three off-diagonal quark Green functions. We call the sum of these two diagrams

$$\Sigma^{(2)+-}_{\text{quark-quark}}(X,p) = \Sigma^{(2)+-}_{\text{E,b)}}(X,p) + \Sigma^{(2)+-}_{\text{QL,a)}}(X,p) \quad (46)$$

and collect the remaining five graphs in the construct

$$\begin{aligned}\Sigma^{(2)+-}_{\text{quark-gluon}}(X,p) &= \Sigma^{(2)+-}_{\text{R,a)}}(X,p) + \Sigma^{(2)+-}_{\text{L,a)}}(X,p) \\ &+\Sigma^{(2)+-}_{\text{C,a)}}(X,p) + \Sigma^{(2)+-}_{\text{C,b)}}(X,p) + \Sigma^{(2)+-}_{\text{E,a)}}(X,p). \quad (47)\end{aligned}$$

This subdivision in eqs. (46) and (47) to $J^{(2)\text{loss}}_{\text{coll}}$ will be handled separately, as the first term will be seen to lead to elastic quark-quark and quark-antiquark differential scattering cross-sections in the transport equation, while the $\Sigma_{\text{quark-gluon}}$ term will be seen to lead to processes involving gluons, such as the processes $q\bar{q} \to gg$ and $qg \to qg$.

5.1.1 Quark-quark and quark-antiquark scattering cross-sections.

Explicit expressions for the quark-loop and its exchange diagram self-energies required in eq. (46) are obtained as

$$\begin{aligned}\Sigma^{(2)+-}_{\text{QL,a)}}(X,p) = -g^4 m^4 F^2_{\text{QL}} \int \frac{\mathrm{d}^4p_1}{(2\pi)^4}\frac{\mathrm{d}^4p_2}{(2\pi)^4}\frac{\mathrm{d}^4p_3}{(2\pi)^4}\frac{\mathrm{d}^4p_4}{(2\pi)^4} \\ \times(2\pi)^4\delta^{(4)}(p-p_1-p_2) \\ \times(2\pi)^4\delta^{(4)}(p_2-p_3+p_4)\, S^{+-}(X,p_1)\, G^{++}(X,p_2) \\ \times S^{+-}(X,p_3)\, S^{-+}(X,p_4)\, G^{--}(X,p_2) \quad (48)\end{aligned}$$

and

$$\begin{aligned}\Sigma^{(2)+-}_{\text{E,b)}}(X,p) = -g^4 m^4 F^2_{\text{E}} \int \frac{\mathrm{d}^4p_1}{(2\pi)^4}\frac{\mathrm{d}^4p_2}{(2\pi)^4}\frac{\mathrm{d}^4p_3}{(2\pi)^4}\frac{\mathrm{d}^4p_4}{(2\pi)^4} \\ \times(2\pi)^4\delta^{(4)}(p-p_1-p_2) \\ \times(2\pi)^4\delta^{(4)}(p_2-p_3+p_4)\, S^{+-}(X,p_1)\, G^{--}(X,p_2) \\ \times S^{+-}(X,p_3)\, S^{-+}(X,p_4)\, G^{++}(X,p-p_3), \quad (49)\end{aligned}$$

where F_{QL} and F_{E} are color factors, that will be given explicitly in appendix C. Since they do not affect our argument, we suppress them in the following.

The collision integral for loss from eq. (27) can be directly evaluated, to give the quark-loop and exchange contributions

$$\begin{aligned}J^{(2)\text{loss}}_{\text{coll},q} = ig^4m^4\frac{\pi}{E_p}\int \frac{\mathrm{d}^4p_1}{(2\pi)^4}\frac{\mathrm{d}^4p_2}{(2\pi)^4}\frac{\mathrm{d}^4p_3}{(2\pi)^4}\frac{\mathrm{d}^4p_4}{(2\pi)^4} \\ \times(2\pi)^8\delta^{(4)}(p-p_1-p_2)\delta^{(4)}(p_2-p_3+p_4) \\ \times\left\{G^{++}(X,p_2)G^{--}(X,p_2)\right. \\ \left.+G^{--}(X,p_2)G^{++}(X,p-p_3)\right\} \\ \times\left(-i\frac{\pi}{E_1}\right)\left(-i\frac{\pi}{E_3}\right)\left(-i\frac{\pi}{E_4}\right)\sum_{i=1}^{8}T_i, \quad (50)\end{aligned}$$

where

$$\begin{aligned}T_1 &= \delta(E_1+p_1^0)\,\delta(E_3+p_3^0) \\ &\quad\times\delta(E_4+p_4^0)\, f_{\bar{q}}(-p_1)\, f_{\bar{q}}(-p_3)\, \bar{f}_{\bar{q}}(-p_4)\, f_q(\vec{p})\,, \\ T_2 &= \delta(E_1+p_1^0)\,\delta(E_3+p_3^0) \\ &\quad\times\delta(E_4-p_4^0)\, f_{\bar{q}}(-p_1)\, f_{\bar{q}}(-p_3)\, f_q(p_4)\, f_q(\vec{p})\,, \\ T_3 &= \delta(E_1+p_1^0)\,\delta(E_3-p_3^0) \\ &\quad\times\delta(E_4+p_4^0)\, f_{\bar{q}}(-p_1)\, \bar{f}_q(p_3)\, \bar{f}_{\bar{q}}(-p_4)\, f_q(\vec{p})\,, \\ T_4 &= \delta(E_1+p_1^0)\,\delta(E_3-p_3^0) \\ &\quad\times\delta(E_4-p_4^0)\, f_{\bar{q}}(-p_1)\, \bar{f}_q(p_3)\, f_q(p_4)\, f_q(\vec{p})\,, \\ T_5 &= \delta(E_1-p_1^0)\,\delta(E_3+p_3^0) \\ &\quad\times\delta(E_4+p_4^0)\, \bar{f}_q(p_1)\, f_{\bar{q}}(-p_3)\, \bar{f}_{\bar{q}}(-p_4)\, f_q(\vec{p})\,, \\ T_6 &= \delta(E_1-p_1^0)\,\delta(E_3+p_3^0) \\ &\quad\times\delta(E_4-p_4^0)\, \bar{f}_q(p_1)\, f_{\bar{q}}(-p_3)\, f_q(p_4)\, f_q(\vec{p})\,, \\ T_7 &= \delta(E_1-p_1^0)\,\delta(E_3-p_3^0) \\ &\quad\times\delta(E_4+p_4^0)\, \bar{f}_q(p_1)\, \bar{f}_q(p_3)\, \bar{f}_{\bar{q}}(-p_4)\, f_q(\vec{p})\,, \\ T_8 &= \delta(E_1-p_1^0)\,\delta(E_3-p_3^0) \\ &\quad\times\delta(E_4-p_4^0)\, \bar{f}_q(p_1)\, \bar{f}_q(p_3)\, f_q(p_4)\, f_q(\vec{p})\,. \quad (51)\end{aligned}$$

One sees that there are eight terms, or eight processes in this expression. However, due to energy momentum conservation T_1, T_2, T_4, T_6 and T_7 vanish, leaving only T_3, T_5 and T_8. This is a direct consequence of the on-shell nature of the quasiparticle approximation. If this were relaxed, all terms would necessarily have to be included.

We can reorganize this expression into a recognizable physical form by making some simple manipulations. Letting $p_i \to -p_i$ for the antiquark states and performing the p_1^0, p_3^0, p_4^0 and the p_2 integration by absorbing the appro-

priate δ-functions, we obtain

$$
\begin{aligned}
J^{(2)\mathrm{loss}}_{\mathrm{coll},q} = & -g^4 m^4 \frac{\pi}{E_p} \int \frac{\mathrm{d}^3 p_1}{(2\pi)^3 2E_1} \frac{\mathrm{d}^3 p_3}{(2\pi)^3 2E_3} \frac{\mathrm{d}^3 p_4}{(2\pi)^3 2E_4} (2\pi)^4 \\
& \times \big\{ \delta^{(4)}(p + p_1 - p_3 - p_4)\, f_{\bar{q}}(\vec{p}_1)\, \bar{f}_q(\vec{p}_3)\, \bar{f}_{\bar{q}}(\vec{p}_4)\, f_q(\vec{p}) \\
& \times \big[G^{++}(X, p + p_1) G^{--}(X, p + p_1) \\
& + G^{--}(X, p + p_1) G^{++}(X, p - p_3) \big] \\
& + \delta^{(4)}(p - p_1 + p_3 - p_4)\, \bar{f}_q(\vec{p}_1)\, f_{\bar{q}}(\vec{p}_3)\, \bar{f}_{\bar{q}}(\vec{p}_4)\, f_q(\vec{p}) \\
& \times \big[G^{++}(X, p - p_1) G^{--}(X, p - p_1) \\
& + G^{--}(X, p - p_1) G^{++}(X, p + p_3) \big] \\
& + \delta^{(4)}(p - p_1 - p_3 + p_4)\, \bar{f}_q(\vec{p}_1)\, \bar{f}_q(\vec{p}_3)\, f_q(\vec{p}_4)\, f_q(\vec{p}) \\
& \times \big[G^{++}(X, p - p_1) G^{--}(X, p - p_1) \\
& + G^{--}(X, p - p_1) G^{++}(X, p - p_3) \big] \big\} . \qquad (52)
\end{aligned}
$$

The first two terms of this expression can be combined if one makes the substitution $p_1 \leftrightarrow p_3$ in the second term. The third term has a symmetry in p_1 and p_3 and can be rewritten as one half the sum of two terms with p_1 and p_3 interchanged. The loss term then becomes

$$
\begin{aligned}
J^{(2)\mathrm{loss}}_{\mathrm{coll},q} = & -g^4 m^4 \frac{\pi}{E_p} \int \frac{\mathrm{d}^3 p_1}{(2\pi)^3 2E_1} \frac{\mathrm{d}^3 p_3}{(2\pi)^3 2E_3} \frac{\mathrm{d}^3 p_4}{(2\pi)^3 2E_4} (2\pi)^4 \\
& \times \big\{ \delta^{(4)}(p + p_1 - p_3 - p_4)\, f_{\bar{q}}(\vec{p}_1)\, \bar{f}_q(\vec{p}_3)\, \bar{f}_{\bar{q}}(\vec{p}_4)\, f_q(\vec{p}) \\
& \times \big[G^{++}(X, p + p_1) G^{--}(X, p + p_1) \\
& + G^{--}(X, p + p_1) G^{++}(X, p - p_3) \\
& + G^{++}(X, p - p_3) G^{--}(X, p - p_3) \\
& + G^{--}(X, p - p_3) G^{++}(X, p + p_1) \big] \\
& + \delta^{(4)}(p - p_1 - p_3 + p_4)\, \bar{f}_q(\vec{p}_1)\, \bar{f}_q(\vec{p}_3)\, f_q(\vec{p}_4)\, f_q(\vec{p}) \\
& \times \frac{1}{2} \big[G^{++}(X, p - p_1) G^{--}(X, p - p_1) \\
& + G^{--}(X, p - p_1) G^{++}(X, p - p_3) \\
& + G^{++}(X, p - p_3) G^{--}(X, p - p_3) \\
& + G^{--}(X, p - p_3) G^{++}(X, p - p_1) \big] \big\} . \qquad (53)
\end{aligned}
$$

Using the fact that $[iG^{--}(p)]^\dagger = iG^{++}(p)$ and making the substitution $p_1 \leftrightarrow p_4$ in the second term, one is able to identify the absolute values squared of the Green functions occurring in $J^{(2),\mathrm{loss}}_{\mathrm{coll},q}$. One has

$$
\begin{aligned}
J^{(2)\mathrm{loss}}_{\mathrm{coll},q} = & \; g^4 m^4 \frac{\pi}{E_p} \int \frac{\mathrm{d}^3 p_1}{(2\pi)^3 2E_1} \frac{\mathrm{d}^3 p_3}{(2\pi)^3 2E_3} \frac{\mathrm{d}^3 p_4}{(2\pi)^3 2E_4} \\
& \times (2\pi)^4 \delta^{(4)}(p + p_1 - p_3 - p_4) \\
& \times \Big\{ \frac{1}{2} \left| iG^{--}(X, p - p_3) + iG^{--}(X, p - p_4) \right|^2 \\
& \times f_q(\vec{p})\, f_q(\vec{p}_1)\, \bar{f}_q(\vec{p}_3)\, \bar{f}_q(\vec{p}_4) \\
& + \left| iG^{--}(X, p + p_1) + iG^{--}(X, p - p_3) \right|^2 \\
& \times f_q(\vec{p})\, f_{\bar{q}}(\vec{p}_1)\, \bar{f}_q(\vec{p}_3)\, \bar{f}_{\bar{q}}(\vec{p}_4) \Big\} . \qquad (54)
\end{aligned}
$$

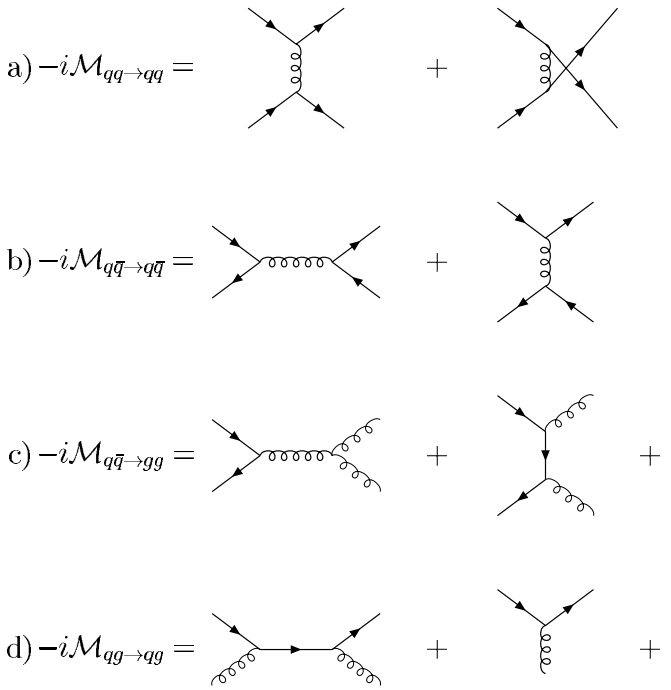

Fig. 7. Feynman diagrams for the matrix element for elastic quark-quark scattering, elastic quark-antiquark scattering, for the process $q\bar{q} \to gg$, and for the process $qg \to qg$.

Now one may recognize the scattering amplitude for elastic quark-quark scattering,

$$
\begin{aligned}
& -i\mathcal{M}_{qq\to qq}(p1 \to 34) = \\
& \quad (-igm)^2 \left[iG^{--}(p - p_3) + iG^{--}(p - p_4) \right] , \qquad (55)
\end{aligned}
$$

and the scattering amplitude for quark-antiquark scattering,

$$
\begin{aligned}
& -i\mathcal{M}_{q\bar{q}\to q\bar{q}}(p1 \to 34) = \\
& \quad (-igm)^2 \left[iG^{--}(p + p_1) + iG^{--}(p - p_3) \right] , \qquad (56)
\end{aligned}
$$

occurring in eq. (54), which may be concisely written as to give the final result

$$
\begin{aligned}
J^{(2)\mathrm{loss}}_{\mathrm{coll},q} = & \; \frac{\pi}{E_p} \int \frac{\mathrm{d}^3 p_1}{(2\pi)^3 2E_1} \frac{\mathrm{d}^3 p_3}{(2\pi)^3 2E_3} \frac{\mathrm{d}^3 p_4}{(2\pi)^3 2E_4} \\
& \times (2\pi)^4 \delta^{(4)}(p + p_1 - p_3 - p_4) \\
& \times \Big\{ \frac{1}{2} \left| \mathcal{M}_{qq\to qq}(p1 \to 34) \right|^2 f_q(\vec{p})\, f_q(\vec{p}_1)\, \bar{f}_q(\vec{p}_3)\, \bar{f}_q(\vec{p}_4) \\
& + \left| \mathcal{M}_{q\bar{q}\to q\bar{q}}(p1 \to 34) \right|^2 f_q(\vec{p})\, f_{\bar{q}}(\vec{p}_1)\, \bar{f}_q(\vec{p}_3)\, \bar{f}_{\bar{q}}(\vec{p}_4) \Big\} . \qquad (57)
\end{aligned}
$$

The Feynman graphs corresponding to these processes are shown in fig. 7 a) and b), respectively.

5.1.2 Quark-gluon scattering cross-sections.

We now turn our attention to the graphs of $\Sigma^{(2)+-}_{\text{quark-gluon}}$ of eq. (47), which will lead to scattering processes that

involve gluonic degrees of freedom. As in the previous section, the Feynman rules for non-equilibrium processes can be applied to these diagrams and the result Wigner transformed. This results in the following expressions for the self-energies:

$$\Sigma^{(2)+-}_{\mathrm{R,a)}}(X,p) = -g^4 m^4 F_{\mathrm{R}}^2 \int \frac{\mathrm{d}^4p_1}{(2\pi)^4}\frac{\mathrm{d}^4p_2}{(2\pi)^4}\frac{\mathrm{d}^4p_3}{(2\pi)^4}\frac{\mathrm{d}^4p_4}{(2\pi)^4}$$
$$\times(2\pi)^4\delta^{(4)}(p-p_1-p_2)$$
$$\times(2\pi)^4\delta^{(4)}(p_2-p_3-p_4)\,G^{+-}(X,p_1)\,S^{++}(X,p-p_3)$$
$$\times G^{+-}(X,p_3)\,S^{+-}(X,p_4)\,S^{--}(X,p-p_3) \qquad (58)$$

for the rainbow diagram,

$$\Sigma^{(2)+-}_{\mathrm{L,a)}}(X,p) = -\frac{1}{2}g^4 m^4 F_{\mathrm{L}}^2 \int \frac{\mathrm{d}^4p_1}{(2\pi)^4}\frac{\mathrm{d}^4p_2}{(2\pi)^4}\frac{\mathrm{d}^4p_3}{(2\pi)^4}\frac{\mathrm{d}^4p_4}{(2\pi)^4}$$
$$\times(2\pi)^4\delta^{(4)}(p-p_1-p_2)$$
$$\times(2\pi)^4\delta^{(4)}(p_2-p_3-p_4)\,G^{+-}(X,p_1)\,G^{++}(X,p_2)$$
$$\times G^{+-}(X,p_3)\,S^{+-}(X,p_4)\,G^{--}(X,p_2) \qquad (59)$$

for the ladder graph,

$$\Sigma^{(2)+-}_{\mathrm{C,a)/b)}}(X,p) = -g^4 m^4 F_{\mathrm{C}}^2 \int \frac{\mathrm{d}^4p_1}{(2\pi)^4}\frac{\mathrm{d}^4p_2}{(2\pi)^4}\frac{\mathrm{d}^4p_3}{(2\pi)^4}\frac{\mathrm{d}^4p_4}{(2\pi)^4}$$
$$\times(2\pi)^4\delta^{(4)}(p-p_1-p_2)$$
$$\times(2\pi)^4\delta^{(4)}(p_2-p_3-p_4)\,G^{+-}(X,p_1)\,G^{\pm\pm}(X,p_2)$$
$$\times G^{+-}(X,p_3)\,S^{+-}(X,p_4)\,S^{\mp\mp}(X,p-p_3) \qquad (60)$$

for the two cloud diagrams, and

$$\Sigma^{(2)+-}_{\mathrm{E,a)}}(X,p) = -g^4 m^4 F_{\mathrm{E}}^2 \int \frac{\mathrm{d}^4p_1}{(2\pi)^4}\frac{\mathrm{d}^4p_2}{(2\pi)^4}\frac{\mathrm{d}^4p_3}{(2\pi)^4}\frac{\mathrm{d}^4p_4}{(2\pi)^4}$$
$$\times(2\pi)^4\delta^{(4)}(p-p_1-p_2)$$
$$\times(2\pi)^4\delta^{(4)}(p_2-p_3-p_4)\,G^{+-}(X,p_1)\,S^{++}(X,p-p_4)$$
$$\times G^{+-}(X,p_3)\,S^{+-}(X,p_4)\,S^{--}(X,p-p_3) \qquad (61)$$

for the first exchange diagram. F_{R}, F_{L}, F_{C} and F_{E} are appropriate color factors, that will be discussed in detail in appendix C, but which will be suppressed here. Note that a factor 1/2 occurs in the expression for the ladder diagram because of the gluon loop. The expressions for $\Sigma^{(2)-+}$ are obtained from the ones for $\Sigma^{(2)+-}$ by exchanging $-$ and $+$. The loss term of eq. (27) incorporating the first rainbow, cloud, ladder and exchange graphs, is given as

$$J^{(2)\mathrm{loss}}_{\mathrm{coll},g} = ig^4 m^4 \frac{\pi}{E_p}\int \frac{\mathrm{d}^4p_1}{(2\pi)^4}\frac{\mathrm{d}^4p_2}{(2\pi)^4}\frac{\mathrm{d}^4p_3}{(2\pi)^4}\frac{\mathrm{d}^4p_4}{(2\pi)^4}$$
$$\times(2\pi)^8\delta^{(4)}(p-p_1-p_2)\delta^{(4)}(p_2-p_3-p_4)$$
$$\times\big\{S^{++}(X,p-p_3)S^{--}(X,p-p_3)$$
$$+\frac{1}{2}G^{++}(X,p_2)G^{--}(X,p_2)$$
$$+G^{++}(X,p_2)S^{--}(X,p-p_3)$$
$$+G^{--}(X,p_2)S^{++}(X,p-p_3)$$
$$+S^{++}(X,p-p_4)S^{--}(X,p-p_3)\big\}$$
$$\times\left(-i\frac{\pi}{E_1}\right)\left(-i\frac{\pi}{E_3}\right)\left(-i\frac{\pi}{E_4}\right)\sum_{i=1}^{8}T_i, \qquad (62)$$

where

$$T_1 = \delta(E_1+p_1^0)\,\delta(E_3+p_3^0)$$
$$\times\delta(E_4+p_4^0)\,f_{\bar q}(-p_1)\,f_{\bar g}(-p_3)\,f_{\bar g}(-p_4)\,f_q(\vec p)\,,$$
$$T_2 = \delta(E_1+p_1^0)\,\delta(E_3+p_3^0)$$
$$\times\delta(E_4-p_4^0)\,f_{\bar q}(-p_1)\,f_{\bar g}(-p_3)\,\bar f_g(p_4)\,f_q(\vec p)\,,$$
$$T_3 = \delta(E_1+p_1^0)\,\delta(E_3-p_3^0)$$
$$\times\delta(E_4+p_4^0)\,f_{\bar q}(-p_1)\,\bar f_g(p_3)\,f_{\bar g}(-p_4)\,f_q(\vec p)\,,$$
$$T_4 = \delta(E_1+p_1^0)\,\delta(E_3-p_3^0)$$
$$\times\delta(E_4-p_4^0)\,f_{\bar q}(-p_1)\,\bar f_g(p_3)\,\bar f_g(p_4)\,f_q(\vec p)\,,$$
$$T_5 = \delta(E_1-p_1^0)\,\delta(E_3+p_3^0)$$
$$\times\delta(E_4+p_4^0)\,\bar f_q(p_1)\,f_{\bar g}(-p_3)\,f_{\bar g}(-p_4)\,f_q(\vec p)\,,$$
$$T_6 = \delta(E_1-p_1^0)\,\delta(E_3+p_3^0)$$
$$\times\delta(E_4-p_4^0)\,\bar f_q(p_1)\,f_{\bar g}(-p_3)\,\bar f_g(p_4)\,f_q(\vec p)\,,$$
$$T_7 = \delta(E_1-p_1^0)\,\delta(E_3-p_3^0)$$
$$\times\delta(E_4+p_4^0)\,\bar f_q(p_1)\,\bar f_g(p_3)\,f_{\bar g}(-p_4)\,f_q(\vec p)\,,$$
$$T_8 = \delta(E_1-p_1^0)\,\delta(E_3-p_3^0)$$
$$\times\delta(E_4-p_4^0)\,\bar f_q(p_1)\,\bar f_g(p_3)\,\bar f_g(p_4)\,f_q(\vec p). \qquad (63)$$

Once again, eight terms result from this multiplication. Now, again due to energy momentum conservation, T_1, T_2, T_3, T_5 and T_8 vanish, and we are left with three non-vanishing terms, T_4, T_6 and T_7.

Applying the same procedure as for $J^{(2)\mathrm{loss}}_{\mathrm{coll},q}$ as in the previous section, one can regroup the remaining terms to read

$$J^{(2)\mathrm{loss}}_{\mathrm{coll},g} = g^4 m^4 \frac{\pi}{E_p}\int \frac{\mathrm{d}^3p_1}{(2\pi)^3 2E_1}\frac{\mathrm{d}^3p_3}{(2\pi)^3 2E_3}\frac{\mathrm{d}^3p_4}{(2\pi)^3 2E_4}$$
$$\times(2\pi)^4\delta^{(4)}(p+p_1-p_3-p_4)$$
$$\times\left\{\frac{1}{2}\left|iG^{--}(X,p+p_1)+iS^{--}(X,p-p_3)\right.\right.$$
$$\left.+iS^{--}(X,p-p_4)\right|^2 f_q(\vec p)\,f_{\bar q}(\vec p_1)\,\bar f_g(\vec p_3)\,\bar f_g(\vec p_4)$$
$$+\left|iS^{--}(X,p+p_1)+iG^{--}(X,p-p_3)\right.$$
$$\left.\left.+iS^{--}(X,p-p_4)\right|^2 f_q(\vec p)\,f_g(\vec p_1)\,\bar f_q(\vec p_3)\,\bar f_g(\vec p_4)\right\}. \qquad (64)$$

In order to identify the physical processes that give rise to these terms, we examine first all possible contributions to the annihilation process $q\bar{q} \to gg$. The Feynman graphs for this within this model are shown in fig. 7 c). The scattering amplitude associated therewith is

$$-i\mathcal{M}_{q\bar{q}\to gg}(p1 \to 34) = (-igm)^2 \times \left[iG^{--}(p+p_1) + iS^{--}(p-p_3) + iS^{--}(p-p_4)\right]. \quad (65)$$

In a similar manner, the elastic scattering process $qg \to qg$, which is shown in fig. 7 d), has the scattering amplitude

$$-i\mathcal{M}_{qg\to qg}(p1 \to 34) = (-igm)^2 \times \left[iS^{--}(p+p_1) + iG^{--}(p-p_3) + iS^{--}(p-p_4)\right]. \quad (66)$$

One can identify the absolute value squared of eqs. (65) and (66) in eq. (64) and therefore $J^{(2)\text{loss}}_{\text{coll},g}$ can be written as

$$J^{(2)\text{loss}}_{\text{coll},g} = \frac{\pi}{E_p}\int \frac{\mathrm{d}^3p_1}{(2\pi)^3 2E_1}\frac{\mathrm{d}^3p_3}{(2\pi)^3 2E_3}\frac{\mathrm{d}^3p_4}{(2\pi)^3 2E_4} \times(2\pi)^4\delta^{(4)}(p+p_1-p_3-p_4) \times\left\{\frac{1}{2}\left|\mathcal{M}_{q\bar{q}\to gg}(p1\to 34)\right|^2 f_q(\vec{p})\, f_{\bar{q}}(\vec{p}_1)\, \bar{f}_g(\vec{p}_3)\, \bar{f}_g(\vec{p}_4)\right. + \left.\left|\mathcal{M}_{qg\to qg}(p1\to 34)\right|^2 f_q(\vec{p}) f_g(\vec{p}_1)\bar{f}_q(\vec{p}_3)\bar{f}_g(\vec{p}_4)\right\}. \quad (67)$$

The complete loss term is obtained by adding eq. (57) and (67),

$$J^{(2)\text{loss}}_{\text{coll}} = J^{(2)\text{loss}}_{\text{coll},q} + J^{(2)\text{loss}}_{\text{coll},g}. \quad (68)$$

The gain term can be constructed by replacing $f \leftrightarrow \bar{f}$ in the complete loss term. With the relation

$$\frac{\mathrm{d}\sigma}{\mathrm{d}\Omega} = \frac{|\mathcal{M}|^2}{|\vec{v}_p - \vec{v}_1|2E_p 2E_1}\frac{\mathrm{d}Q}{\mathrm{d}\Omega} \quad (69)$$

and the phase space factor

$$Q = (2\pi)^4\delta^{(4)}(p+p_1-p_3-p_4)\frac{\mathrm{d}^3p_3}{(2\pi)^3 2E_3}\frac{\mathrm{d}^3p_4}{(2\pi)^3 2E_4}, \quad (70)$$

the final form for the Boltzmann equation, calculated for two-loop self-energy graphs, is for quarks ($a = q$)

$$2p\partial_X f_a(X,\vec{p}) = \int \mathrm{d}\Omega \frac{\mathrm{d}^3p_1}{(2\pi)^3 2E_1}|\vec{v}_p - \vec{v}_1|2E_p 2E_1 \times\sum_{j=1}^{4} s_j \frac{\mathrm{d}\sigma_j}{\mathrm{d}\Omega}\bigg|_{ab\to cd}\left[\bar{f}_a(\vec{p})\bar{f}_b(\vec{p}_1)f_c(\vec{p}_3)f_d(\vec{p}_4) - f_a(\vec{p})f_b(\vec{p}_1)\bar{f}_c(\vec{p}_3)\bar{f}_d(\vec{p}_4)\right], \quad (71)$$

where partons b, c, and d can be a quark, antiquark or gluon, and j labels the four processes $j = 1...4$ corresponding to $q\bar{q} \to gg$, $qg \to qg$, $qq \to qq$ and $q\bar{q} \to q\bar{q}$. The s_j are symmetry factors $s_1 = s_3 = 1/2$ and $s_2 = s_4 = 1$.

The transport equation for gluons can be obtained in an analogous way and calculated for two loops, it takes the same form as eq. (71) with $a = g$. Then j labels the four processes $j = 1...4$ corresponding to $gg \to gg$, $gg \to q\bar{q}$, $gq \to gq$ and $g\bar{q} \to g\bar{q}$. The appropriate symmetry factors are $s_1 = 1/2$ and $s_2 = s_3 = s_4 = 1$.

5.2 Higher-order corrections to the process $q\bar{q} \to g$

Now, we wish to demonstrate precisely that the remaining two-loop graphs contribute to corrections of order g^3m^3 to the lower-order process $q\bar{q} \to g$. To demonstrate this, we arbitrarily examine the set of quark-loop diagrams. The QL a) graph of fig. 6 leads directly to the qq and $q\bar{q}$ cross-sections of fig. 7 a) and b), while the three graphs, QL b)-d) of fig. 6 were *not* required for the evaluation of these cross-sections. We notice that the quark-loop self-energy graphs contain a self-energy insertion which is just the gluonic Fock self-energy shown in fig. 5(b). To simplify our notations, we call it in the following $\Pi^{ij}(X,k)$ and it reads as

$$-i\Pi^{ij}(X,k) := (-)^{i+j}(igm)^2 \times\int\frac{\mathrm{d}^4l}{(2\pi)^4} iS^{ij}(X,k+l)\, iS^{ji}(X,l), \quad (72)$$

where the color factor is suppressed. Here $i,j = +,-$ and $(-)^{i+j} = +1$ (-1) for $i = j$ $(i \neq j)$.

We commence now with the diagram QL b) of fig. 6 which is given by

$$-i\Sigma^{(2)+-}_{\text{QL,b)}}(X,p) = g^2m^2F^2_{\text{QL}}\int\frac{\mathrm{d}^4p_1}{(2\pi)^4}\frac{\mathrm{d}^4p_2}{(2\pi)^4} \times(2\pi)^4\delta^{(4)}(p-p_1-p_2)\, iS^{+-}(X,p_1) \times iG^{+-}(X,p_2)\,(-i\Pi^{++}(X,p_2))iG^{++}(X,p_2), \quad (73)$$

where F^2_{QL} is again the color factor given in eq. (C.12). The corresponding loss term of the collision integral of eq. (27) to this self-energy reads as

$$J^{(2)\text{loss}}_{\text{coll,QL,b)}} = -i\frac{\pi}{E_p}\Sigma^{(2)+-}_{\text{QL,b)}}(X,p^0 = E_p,\vec{p})f_q(X,\vec{p}). \quad (74)$$

In this expression, the product $iS^{+-}(X,p_1)iG^{+-}(X,p_2)f_q(X,\vec{p})$ occurs. Inserting the quasiparticle approximation for the Green functions of eqs. (20) and (21), we obtain for this product the sum of four terms:

$$\begin{aligned}
T_1 &= \frac{\pi}{E_1}\frac{\pi}{E_2}\delta(E_1-p_1^0)\delta(E_2-p_2^0) \times\bar{f}_q(X,p_1)\bar{f}_g(X,p_2)f_q(X,\vec{p}),\\
T_2 &= \frac{\pi}{E_1}\frac{\pi}{E_2}\delta(E_1-p_1^0)\delta(E_2+p_2^0) \times\bar{f}_q(X,p_1)f_g(X,-p_2)f_q(X,\vec{p}),\\
T_3 &= \frac{\pi}{E_1}\frac{\pi}{E_2}\delta(E_1+p_1^0)\delta(E_2-p_2^0) \times f_{\bar{q}}(X,-p_1)\bar{f}_g(X,p_2)f_q(X,\vec{p}),\\
T_4 &= \frac{\pi}{E_1}\frac{\pi}{E_2}\delta(E_1+p_1^0)\delta(E_2+p_2^0) \times f_{\bar{q}}(X,-p_1)f_g(X,-p_2)f_q(X,\vec{p}).
\end{aligned} \quad (75)$$

By attributing again f to incoming particles and $\bar{f}$ to outgoing ones, we see that $T_1...T_4$ correspond to the processes $q \to qg$, $qg \to q$, $q\bar{q} \to g$ and $q\bar{q}g \to \emptyset$. Since the quarks are massless, while the gluons are endowed with a finite mass, the processes corresponding

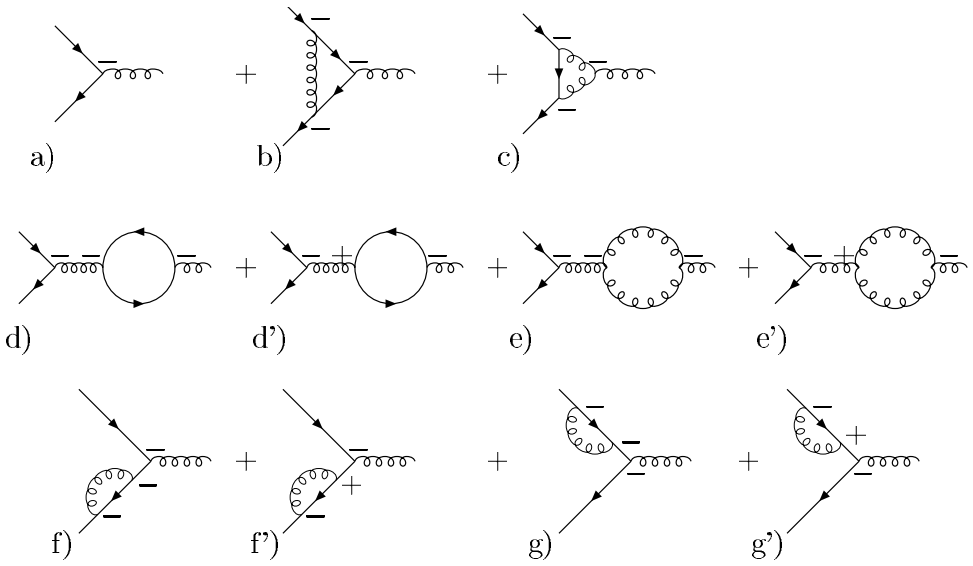

Fig. 8. The process $q\bar{q} \to g$ up to order $(gm)^3$.

to T_1, T_2 and T_4 are kinematically forbidden as also occurred in the discussion of the Fock term in subsect. 4.2. One thus has one remaining non-vanishing contribution $iS^{+-}(X,p_1)iG^{+-}(X,p_2)f_q(X,\vec{p}) = T_3$. This product is now inserted into eq. (74). In the resulting expression, we interchange p_1 with $-p_1$ and on performing the p_1^0 and p_2^0 integrations, we find the result

$$J^{(2)\mathrm{loss}}_{\mathrm{coll,QL,b)}} = -\frac{\pi}{E_p} g^2 m^2 F^2_{\mathrm{QL}} \int \frac{\mathrm{d}^3p_1}{(2\pi)^3 2E_1} \frac{\mathrm{d}^3p_2}{(2\pi)^3 2E_2} \times(2\pi)^4\delta^{(4)}(p+p_1-p_2) \times G^{++}(X,p_2)\, \Pi^{++}(X,p_2) \times f_{\bar{q}}(X,\vec{p}_1)\bar{f}_g(X,\vec{p}_2) f_q(X,\vec{p}) \quad (76)$$

as the remaining contribution of the QL b) graph to the collision integral.

Since T_3 corresponds to the process $q\bar{q} \to g$ which has also come to the fare in sect. 4, we would like to take a closer look at this process. In fig. 8, all Feynman diagrams for this process are shown up to order g^3m^3. As mentioned in appendix A, the vertices linked to external lines are $s = -$ ("physical fields"), while the inner vertices can be of type $-$ or $+$ and one has to include all possibilities. That leads to a doubling of the diagrams with inner vertices and we obtain, in addition to the diagrams which one has in $T = 0$ equilibrium field theory, *i.e.* diagrams with only $-$ vertices, (in our case graph a), b), c), d), e), f) and g)), also diagrams with one $+$ vertex, *i.e.* in our case graph d′), e′), f′) and g′).

The scattering amplitude associated with fig. 8a) has purely a point-like structure with color groups occurring:

$$-i\mathcal{M}^{a)}_{q\bar{q}\to g} = -igmt^a_{ij} \otimes t^r_{lm}\,, \quad (77)$$

while from fig. 8d), one has

$$-i\mathcal{M}^{d)}_{q\bar{q}\to g} = -igm[t^b_{ji}\mathrm{tr}(t^b t^a)] \otimes [t^s_{ml}\mathrm{tr}(t^s t^r)]\, G^{--}(X,p_2)\, \Pi^{--}(X,p_2), \quad (78)$$

where t^a_{ij} is the matrix of the color group in the representation of the quarks. Now note that using the fact that $[iG^{--}]^\dagger = iG^{++}$ and $F_{\mathrm{QL}} = t^a_{ij}t^b_{ji}\mathrm{tr}(t^b t^a)$, one can rewrite eq. (76) in terms of these matrix elements, *i.e.*

$$J^{(2)\mathrm{loss}}_{\mathrm{coll,QL,b)}} = \frac{\pi}{E_p} \int \frac{\mathrm{d}^3p_1}{(2\pi)^3 2E_1} \frac{\mathrm{d}^3p_2}{(2\pi)^3 2E_2} (2\pi)^4\delta^{(4)}(p+p_1-p_2) \times \mathcal{M}^{a)}_{q\bar{q}\to g}[\mathcal{M}^{d)}_{q\bar{q}\to g}]^\dagger f_q(X,\vec{p}) f_{\bar{q}}(X,\vec{p}_1)\bar{f}_g(X,\vec{p}_2), \quad (79)$$

illustrating that the cross term between these two processes, denoted symbolically as $ad^\dagger$, is derived from the self-energy diagram QL b) of fig. 6. The gain term can be obtained by replacing f with $\bar{f}$ and vice versa in eq. (79).

In a similar fashion, the collision integral can be constructed from the quark-loop diagram QL c) in fig. 6. One obtains an expression for the loss term as in eq. (76) with $G^{++}\,\Pi^{++}$ replaced by the combination $G^{--}\,\Pi^{--}$. Again $J^{(2)\mathrm{loss}}_{\mathrm{coll,QL,c)}}$ can be expressed by the scattering amplitudes of eq. (77) and (78):

$$J^{(2)\mathrm{loss}}_{\mathrm{coll,QL,c)}} = \frac{\pi}{E_p} \int \frac{\mathrm{d}^3p_1}{(2\pi)^3 2E_1} \frac{\mathrm{d}^3p_2}{(2\pi)^3 2E_2} (2\pi)^4\delta^{(4)}(p+p_1-p_2) \times [\mathcal{M}^{a)}_{q\bar{q}\to g}]^\dagger \mathcal{M}^{d)}_{q\bar{q}\to g} f_q(X,\vec{p}) f_{\bar{q}}(X,\vec{p}_1)\bar{f}_g(X,\vec{p}_2), \quad (80)$$

i.e. the second cross term $a^\dagger d$ required in building a cross-section of the basic component a) and d) of fig. 8 is obtained.

In an analogous fashion, one can show that the rainbow diagrams R b) and c) lead to a collision integral containing $\mathcal{M}^{a)}_{q\bar{q}\to g}[\mathcal{M}^{f)}_{q\bar{q}\to g}]^\dagger$ and the Hermitian conjugate of this product, the ladder diagrams Lb) and c) to a collision integral containing $\mathcal{M}^{a)}_{q\bar{q}\to g}[\mathcal{M}^{e)}_{q\bar{q}\to g}]^\dagger$ and its Hermitian conjugate, the cloud diagrams C c) and d) to a collision integral containing $\mathcal{M}^{a)}_{q\bar{q}\to g}[\mathcal{M}^{c)}_{q\bar{q}\to g}]^\dagger$ and its Hermitian conjugate, and finally the exchange diagrams E c) and d) to a collision integral containing $\mathcal{M}^{a)}_{q\bar{q}\to g}[\mathcal{M}^{b)}_{q\bar{q}\to g}]^\dagger$ and its Hermitian conjugate.

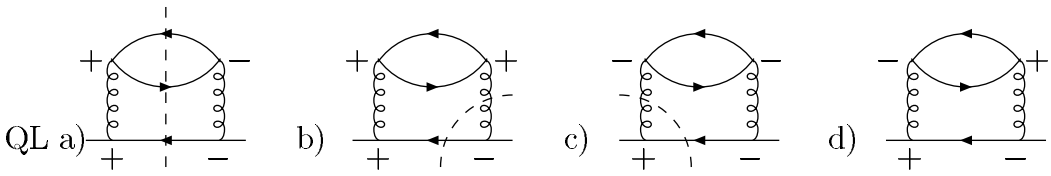

Fig. 9. Quark-loop self-energy diagrams with cut lines (dashed lines).

Note that if we would have only "physical" fields, *i.e.* only − vertices, then we would be able to account for all mixed diagrams that would occur in the construction of the $|\mathcal{M}_{q\bar{q}\to g}|^2$ up to order g^4m^4, with the exception of the diagram g) of fig. 8. This graph does not enter into the collision integral, as it is a renormalization diagram for the *incoming* quark, for which the momentum p is fixed externally.

Returning to our explicit example of the quark-loop self-energy of fig. 6, one sees that a simple graphical interpretation can be applied to each figure which we have considered so far. A rule in which all lines that are connected by $\pm$ and $\mp$ are cut in a single path, separates the graphs QL a) to c) into their component matrix elements. This is illustrated in fig. 9. This procedure, however, cannot be applied uniquely to the graph QL d), nor for that matter to the remaining graphs which are not required for construction of the mixed terms or direct contributions to the cross-sections, *i.e.* the graphs R d) and L d). We are thus now left with the three graphs QL d), R d) and L d) which at first sight fit into no apparent scheme, and which therefore may present difficulties.

We commence with the investigation of L d). To each of the three-gluon vertices are associated three off-diagonal gluonic Green functions. Due to the quasiparticle approximation, they have to be on-shell. Therefore each three-gluon vertex corresponds to a on-shell process of a (massive) gluon decaying into two (massive) gluons which is forbidden. For this reason, the diagram L d) vanishes.

For the graphs QL d) and R d), the situation is different. For QL d) we obtain an expression as in eq. (73) with the product of the five Green functions replaced by $S^{+-}(X,p_1)[G^{+-}(X,p_2)]^2S^{-+}(X,p_3)S^{+-}(X,p_4)$. In the quasiparticle approximation the off-diagonal Green functions are on mass shell:

$$p_1^2 = p_3^2 = p_4^2 = 0\,, \tag{81}$$

$$p_2^2 = m^2\,. \tag{82}$$

In addition to this, the two δ-functions for the energy momentum conservation of eq. (73) have to be fulfilled. Therefore we can write for example

$$0 = p_3^2 = (p_2+p_4)^2 = 2p_2p_4 + m^2. \tag{83}$$

One possible choice which fulfills these equations is

$$p_2 = (m,0) \quad \text{and} \quad p_4 = (-m/2, m/2). \tag{84}$$

Here and in the following, the first component denotes the energy and the second one the value of the three momentum leaving its direction arbitrary. From this one obtains $p_3 = p_2 + p_4 = (m/2, m/2)$ which is on its mass shell.

Thus we are left with the two graphs QL d) and R d). Our task is now to rewrite these self-energies in terms of a scattering product. We were able to express all other self-energy graphs of fig. 6 in terms of scattering amplitudes and saw afterwards, that this corresponds to the cutting of all off-diagonal propagators. But for the graphs QL d) and R d) we cannot use this cutting rule, since each graph consists of five off-diagonal propagators and therefore cannot be cut in an obvious and unique way. Note that the cutting rule must be derived as a consequence of a calculation and serves in hindsight as an aid.

On the other hand, to obtain $|\mathcal{M}_{q\bar{q}\to g}|^2$ up to order g^4m^4 correctly, we still have to consider the scattering amplitudes shown in fig. 8 d′), e′) and f′). Since g′) is again a renormalization graph for the incoming quark with fixed momentum, we do not have to consider it. Let us first note that diagram e′) vanishes for the same reason as the self-energy graph L d): the inner vertex corresponds to the (on-shell) decay of a massive particle into two (on-shell) particles of the same species which is forbidden. For this reason, we still need the products $\mathcal{M}^{a)}_{q\bar{q}\to g}[\mathcal{M}^{d')}_{q\bar{q}\to g}]^\dagger$, $\mathcal{M}^{a)}_{q\bar{q}\to g}[\mathcal{M}^{f')}_{q\bar{q}\to g}]^\dagger$ and their Hermitian conjugates.

As mentioned in appendix A, to obtain the absolute square of a scattering amplitude, one needs the scattering amplitude times its Hermitian conjugate in *position* space. The latter is obtained from the original scattering amplitude by interchanging − with + vertices and vice versa [23]. So far, we have considered only scattering amplitudes containing − vertices only, for which the Hermitian conjugate in position space, *i.e.* the same amplitude but all vertices are +, is also the Hermitian conjugate in momentum space, since $[iD^{--}]^\dagger = iD^{++}$ and $(-igm)^\dagger = +igm$. But now we have to consider scattering amplitudes containing both types of vertices, and this difference therefore matters.

After we have clarified the meaning of Hermitian conjugation, we take a closer look at the diagram QL d) of fig. 6.

As before, we obtain an expression for the loss term as in eq. (76) with $G^{++}\,\Pi^{++}$ replaced by $G^{+-}\,\Pi^{-+}$ to read as

$$\begin{aligned} -i\Sigma^{(2)+-}_{\mathrm{QL,d)}}(X,p) = g^2m^2F^2_{\mathrm{QL}} \int \frac{\mathrm{d}^4p_1}{(2\pi)^4}\frac{\mathrm{d}^4p_2}{(2\pi)^4} \\ \times(2\pi)^4\delta^{(4)}(p-p_1-p_2)\,iS^{+-}(X,p_1) \\ \times iG^{+-}(X,p_2)\,(-i\Pi^{-+}(X,p_2))iG^{+-}(X,p_2). \end{aligned} \tag{85}$$

On the other hand, the scattering amplitude of fig. 8d′) is given by

$$-i\mathcal{M}^{d')}_{q\bar{q}\to g} = -igm[t^b_{ji}\mathrm{tr}(t^b t^a)] \otimes[t^s_{ml}\mathrm{tr}(t^s t^r)]\, G^{+-}(X,p_2)\, \Pi^{-+}(X,p_2). \quad (86)$$

Therefore one can express $J^{(2)\mathrm{loss}}_{\mathrm{coll,QL,d)}}$ by the scattering amplitudes of eq. (77) and (86):

$$J^{(2)\mathrm{loss}}_{\mathrm{coll,QL,d)}} = \frac{\pi}{E_p}\int \frac{d^3p_1}{(2\pi)^3 2E_1}\frac{d^3p_2}{(2\pi)^3 2E_2} \times(2\pi)^4\delta^{(4)}(p+p_1-p_2) \times[\mathcal{M}^{a)}_{q\bar{q}\to g}]^\dagger \mathcal{M}^{d')}_{q\bar{q}\to g} f_q(X,\vec{p}) f_{\bar{q}}(X,\vec{p}_1)\bar{f}_g(X,\vec{p}_2). \quad (87)$$

Note that it is *not* possible to express $J^{(2)\mathrm{loss}}_{\mathrm{coll,QL,d)}}$ in terms of $\mathcal{M}^{a)}_{q\bar{q}\to g}\,[\mathcal{M}^{d')}_{q\bar{q}\to g}]^\dagger$. The latter amplitude is obtained from the graph in fig. 8d′) by replacing all − vertices with + vertices and vice versa. It reads

$$[-i\mathcal{M}^{d')}_{q\bar{q}\to g}]^\dagger = igm[t^b_{ji}\mathrm{tr}(t^b t^a)] \otimes[t^s_{ml}\mathrm{tr}(t^s t^r)]\, G^{-+}(X,p_2)\, \Pi^{+-}(X,p_2). \quad (88)$$

Since in eq. (85) p_2 is integrated over, we are free to replace p_2 by $-p_2$. Noting that $G^{+-}(X,-p_2) = G^{-+}(X,p_2)$ and $\Pi^{-+}(X,-p_2) = \Pi^{+-}(X,p_2)$, we obtain an expression which superficially resembles the one in eq. (88). However, on the other hand, the second $G^{+-}(X,-p_2)$ yields a factor $\bar{f}_g(X,-p_2)$ which does not correspond to the process $[-i\mathcal{M}^{d')}_{q\bar{q}\to g}]^\dagger$, for which a gluon with momentum $+p_2$ is outgoing.

In a similar fashion, one can show that the remaining rainbow graph R d) of fig. 6 leads to a collision integral containing $[\mathcal{M}^{a)}_{q\bar{q}\to g}]^\dagger\,\mathcal{M}^{f')}_{q\bar{q}\to g}$. A collision integral containing the Hermitian conjugate term $\mathcal{M}^{a)}_{q\bar{q}\to g}\,\mathcal{M}^{f')}_{q\bar{q}\to g}]^\dagger$ is not obvious, but is in fact present. This is discussed in the following section.

We compare this result with real-time thermal field theory for which cutting rules were derived in the '80s by Kobes and Semenoff [24,25] and in the '90s by Bedaque, Das, and Naik [26] (for a comparison of these two approaches see [27]). Kobes and Semenoff investigated in [25] self-energy graphs with one type of particles. For the two-loop self-energy graph containing a self-energy insertion (corresponding, *e.g.*, to our quark-loop graph with only one type of particles) they found that three graphs can be cut as shown in fig. 9 and can be interpreted in terms of products of scattering amplitudes, while the last graph (in our case $\Sigma^{+-}_{\mathrm{QL,d)}}$) cannot be cut, but corresponds to a product of scattering amplitudes of which one contains a + vertex (in our case this is the product $a^\dagger d'$). To this extent, their result is similar to ours. They concluded that decay amplitudes with only − vertices correspond directly to specific cuts of the associated self-energy graph while decay amplitudes containing some + vertices correspond to self-energy graphs which are not cuttable. They did not state that one product (*i.e.* in our case $a\,d'^\dagger$) is missing nor is an explanation given for this.

For the derivation of the cutting rules of Bedaque *et al.*, the KMS relation was used and can therefore not be generalized directly for non-equilibrium systems. In their approach all "uncuttable" graphs cancel when a summation over the internal vertices ($s = -,+$) is performed. The discrepancy with the approach of Kobes and Semenoff lies in the difference in definition of the propagators which are to be cut. A closer analysis of Gelis [27] has revealed that uncuttable graphs in the sense of Kobes and Semenoff are hidden in the cuttable graphs of Bedaque *et al.* As an example, they have investigated the two-loop self-energy graphs with a vertex correction (these graphs correspond to our cloud graphs with only one type of particles). But these graphs are problem-free anyway and they have found the same products of scattering amplitudes as we have.

Let us conclude this section by commenting that the collision integral constructed from a first set of two-loop self-energy diagrams, *i.e.* the graphs R a), L a), C a) and b), E a) and b), and QL a) of fig. 6, was expressed in terms of all possible $2 \to 2$ cross-sections. The collision integral constructed from the remaining self-energy diagrams of fig. 6 was rewritten in terms of products of scattering amplitudes of the process $q\bar{q} \to g$. In this fashion, however, it is not possible to obtain an absolute square of the sum of amplitudes a) to f′) shown in fig. 8 up to order g^4m^4 since two products, *i.e.* $\mathcal{M}^{a)}_{q\bar{q}\to g}\,[\mathcal{M}^{d')}_{q\bar{q}\to g}]^\dagger$ and $\mathcal{M}^{a)}_{q\bar{q}\to g}\,[\mathcal{M}^{f')}_{q\bar{q}\to g}]^\dagger$ are still missing. We will tackle this issue in the next section.

5.3 Another approach

We found in the last section that it was not possible to obtain an absolute square of the sum of the amplitudes a) - f′) shown in fig. 8 up to order g^4m^4 since two products, *i.e.* $\mathcal{M}^{a)}_{q\bar{q}\to g}\,[\mathcal{M}^{d')}_{q\bar{q}\to g}]^\dagger$ and $\mathcal{M}^{a)}_{q\bar{q}\to g}\,[\mathcal{M}^{f')}_{q\bar{q}\to g}]^\dagger$ are still missing.

For the first product, one requires $[\mathcal{M}^{d')}_{q\bar{q}\to g}]^\dagger$ given in eq. (88). This amplitude contains the self-energy insertion $\Pi^{+-}(X,p_2)$ which cannot be obtained from the self-energy graph $\Sigma^{(2)+-}_{QL,d)}$ as explained in the last section after eq. (88). The only other self-energy graph which could possibly supply this self-energy insertion is obviously $\Sigma^{(2)+-}_{QL,a)}$ of fig. 6. Thus let us look at this graph again in more detail: its contribution to the collision integral reads

$$J^{(2)\mathrm{loss}}_{\mathrm{coll,QL,a)}} = g^2m^2\frac{\pi}{E_p}\int\frac{\mathrm{d}^4p_1}{(2\pi)^4}\frac{\mathrm{d}^4p_2}{(2\pi)^4} \times(2\pi)^4\,\delta^{(4)}(p-p_1-p_2)\,iS^{+-}(X,p_1) \times iG^{--}(X,p_2)\,\left[-i\Pi^{+-}(X,p_2)\right] \times iG^{++}(X,p_2)\,f_q(X,\vec{p}). \quad (89)$$

Here and in the following we suppress the color factors for simplicity. Inserting the quasiparticle approximation $iS^{+-}(X,p_1) = \pi/E_1\{\delta(E_1-p_1^0)\bar{f}_q(X,p_1) + \delta(E_1+p_1^0)f_{\bar{q}}(X,-p_1)\}$ yields two contributions. The first one is

proportional to $\bar{f}_q(X,p_1)$ and is considered later. The second one is proportional to $f_{\bar{q}}(X,-p_1)$ and gives

$$J^{(2)\text{loss }2^{\text{nd}}}_{\text{coll,QL,a)}} = g^2m^2\frac{\pi}{E_p}\int\frac{\mathrm{d}^3p_1}{2E_1(2\pi)^3}\,\frac{\mathrm{d}^4p_2}{(2\pi)^4} \times(2\pi)^4\,\delta^{(3)}(\vec{p}+\vec{p}_1-\vec{p}_2)\,\delta(E_p+E_1-p_2^0) \times iG^{--}(X,p_2)\,\left[-i\Pi^{+-}(X,p_2)\right] \times iG^{++}(X,p_2)\,f_{\bar{q}}(X,\vec{p}_1)\,f_q(X,\vec{p}), \tag{90}$$

where p_1 was substituted by $-p_1$ and the p_1^0-integration was performed. Now we insert the quasiparticle approximation of eqs. (22) and (23) for $G^{\mp\mp}(X,p_2)$. Using the relation

$$\frac{\pm i}{p_2^2-m^2\pm i\epsilon} = \mathsf{P}\frac{\pm i}{p_2^2-m^2} + \pi\delta(p_2^2-m^2) \tag{91}$$

and the fact that

$$\int \mathrm{d}p_2^0\;\mathsf{P}\frac{1}{p_2^2-m^2}\;\delta(E_2\pm p_2^0) = 0, \tag{92}$$

where P denotes the principal value, we find

$$J^{(2)\text{loss }2^{\text{nd}}}_{\text{coll,QL,a)}} = g^2m^2\frac{\pi}{E_p}\int\frac{\mathrm{d}^3p_1}{2E_1(2\pi)^3}\,\frac{\mathrm{d}^4p_2}{(2\pi)^4} \times(2\pi)^4\,\delta^{(3)}(\vec{p}+\vec{p}_1-\vec{p}_2)\,\delta(E_p+E_1-p_2^0)\,\left[-i\Pi^{+-}(X,p_2)\right] \times\left\{\left|\mathsf{P}\frac{i}{p_2^2-m^2}\right|^2+\left[\frac{\pi}{E_2}\delta(E_2-p_2^0)\left(f_g(X,p_2)+\frac{1}{2}\right)\right.\right. \left.\left.+\frac{\pi}{E_2}\delta(E_2+p_2^0)\left(f_g(X,-p_2)+\frac{1}{2}\right)\right]^2\right\} \times f_{\bar{q}}(X,\vec{p}_1)\,f_q(X,\vec{p}). \tag{93}$$

The energy conserving δ-function yields $p_2^0 = E_p + E_1 > 0$. Therefore the term proportional to $\delta(E_2+p_2^0)$ cannot contribute and the term in the curly brackets reads

$$\begin{aligned}
&\left\{\left|\mathsf{P}\frac{i}{p_2^2-m^2}\right|^2+\left[\frac{\pi}{E_2}\delta(E_2-p_2^0)\left(f_g(X,p_2)+\frac{1}{2}\right)\right]^2\right\}\\
&=\left|\mathsf{P}\frac{i}{p_2^2-m^2}\right|^2+\frac{\pi^2}{E_2^2}\delta^2(E_2-p_2^0)\left(f_g(X,p_2)\bar{f}_g(X,p_2)+\frac{1}{4}\right)\\
&=\left|\mathsf{P}\frac{i}{p_2^2-m^2}\right|^2+\frac{\pi}{E_2}\delta(E_2-p_2^0)\bar{f}_g(X,p_2)\\
&\qquad\times\frac{\pi}{E_2}\delta(E_2-p_2^0)f_g(X,p_2)+\left[\frac{\pi}{2E_2}\delta(E_2-p_2^0)\right]^2\\
&=\left|\mathsf{P}\frac{i}{p_2^2-m^2}\right|^2+\frac{\pi}{E_2}\delta(E_2-p_2^0)\bar{f}_g(X,p_2)\\
&\qquad\times\Theta(p_2^0)iG^{-+}(X,p_2)+\left[\pi\Theta(p_2^0)\delta(p_2-m^2)\right]^2\\
&=\left|\frac{i}{p_2^2-m^2+i\epsilon}\right|^2+\frac{\pi}{E_2}\delta(E_2-p_2^0)\bar{f}_g(X,p_2)\;iG^{-+}(X,p_2).
\end{aligned} \tag{94}$$

In the last step we have used $p_2^0>0$ and eqs. (91) and (92). Inserting this expression in eq. (93) gives

$$J^{(2)\text{loss }2^{\text{nd}}}_{\text{coll,QL,a)}} = g^2m^2\frac{\pi}{E_p}\int\frac{\mathrm{d}^3p_1}{2E_1(2\pi)^3}\,\frac{\mathrm{d}^4p_2}{(2\pi)^4} \times(2\pi)^4\,\delta^{(4)}(p+p_1-p_2)\,\left[-i\Pi^{+-}(X,p_2)\right] \times\left\{\left|\frac{i}{p_2^2-m^2+i\epsilon}\right|^2+\frac{\pi}{E_2}\delta(E_2-p_2^0) \times\bar{f}_g(X,p_2)\;iG^{-+}(X,p_2)\right\} f_{\bar{q}}(X,\vec{p}_1)\,f_q(X,\vec{p}). \tag{95}$$

We can express the second term in terms of the scattering amplitude $[-i\mathcal{M}^{d')}_{q\bar{q}\to g}]^\dagger$ of eq. (88) to obtain

$$J^{(2)\text{loss }2^{\text{nd}}}_{\text{coll,QL,a)}} = g^2m^2\frac{\pi}{E_p}\int\frac{\mathrm{d}^3p_1}{2E_1(2\pi)^3}\,\frac{\mathrm{d}^4p_2}{(2\pi)^4} \times(2\pi)^4\,\delta^{(4)}(p+p_1-p_2)\,\left[-i\Pi^{+-}(X,p_2)\right] \times\left|\frac{i}{p_2^2-m^2+i\epsilon}\right|^2\;f_{\bar{q}}(X,\vec{p}_1)\,f_q(X,\vec{p}) +\frac{\pi}{E_p}\int\frac{\mathrm{d}^3p_1}{2E_1(2\pi)^3}\,\frac{\mathrm{d}^3p_2}{2E_2(2\pi)^3}\,(2\pi)^4\,\delta^{(4)}(p+p_1-p_2) \times\mathcal{M}^{a)}_{q\bar{q}\to g}\,[\mathcal{M}^{d')}_{q\bar{q}\to g}]^\dagger\,f_q(X,\vec{p})\,f_{\bar{q}}(X,\vec{p}_1)\,\bar{f}_g(X,\vec{p}_2). \tag{96}$$

Let us comment on this result. The second term gives precisely the contribution we were looking for, *i.e.* the missing product of the scattering amplitudes $\mathcal{M}^{a)}_{q\bar{q}\to g}\,[\mathcal{M}^{d')}_{q\bar{q}\to g}]^\dagger$! The first term however gives the same contribution as eq. (90) with the non-equilibrium propagators $G^{\mp\mp}(X,p_2)$ replaced by the Feynman propagators $G_F^{(*)}(p_2) = (-)i/(p_2^2-m^2\pm i\epsilon)$. Therefore we can make the same manipulations with this term as we did with the first term of eq. (50) in subsubsect. 5.1.1. There, we found that only one term proportional to $f_{\bar{q}}(X,\vec{p}_1)$ contributed to $J^{(2)\text{loss}}_{\text{coll,QL,a)}}$, *i.e.* T_3 of eq. (51). We showed that this term corresponds to the s-channel of the process $q\bar{q}\to q\bar{q}$. Thus, we can rewrite the first term of eq. (96) in a similar fashion to eq. (57) and obtain for eq. (96)

$$J^{(2)\text{loss }2^{\text{nd}}}_{\text{coll,QL,a)}} = \frac{\pi}{E_p}\int\frac{\mathrm{d}^3p_1}{2E_1(2\pi)^3}\,\frac{\mathrm{d}^3p_3}{2E_3(2\pi)^3}\,\frac{\mathrm{d}^3p_4}{2E_4(2\pi)^3} \times(2\pi)^4\,\delta^{(4)}(p+p_1-p_3-p_4) \times\left|\mathcal{M}^{s\text{-channel}}_{q\bar{q}\to q\bar{q}}\right|^2\;f_q(X,\vec{p})\,f_{\bar{q}}(X,\vec{p}_1)\,\bar{f}_q(X,\vec{p}_3)\,\bar{f}_{\bar{q}}(X,\vec{p}_4) +\frac{\pi}{E_p}\int\frac{\mathrm{d}^3p_1}{2E_1(2\pi)^3}\,\frac{\mathrm{d}^3p_2}{2E_2(2\pi)^3}\,(2\pi)^4\,\delta^{(4)}(p+p_1-p_2) \times\mathcal{M}^{a)}_{q\bar{q}\to g}\,[\mathcal{M}^{d')}_{q\bar{q}\to g}]^\dagger\,f_q(X,\vec{p})\,f_{\bar{q}}(X,\vec{p}_1)\,\bar{f}_g(X,\vec{p}_2), \tag{97}$$

where for $\left|\mathcal{M}^{s\text{-channel}}_{q\bar{q}\to q\bar{q}}\right|^2$ the Feynman propagator G_{F} is used. Here, the gluon propagator can be on-mass shell, and the difference between the non-equilibrium propagator G^{--} and the Feynman propagator G_{F} matters.

We consider now the contribution to $J^{(2)\text{loss}}_{\text{coll,QLa)}}$ of eq. (89) given by the first term of iS^{+-} proportional to

$\bar{f}_q(X,p_1)$. We have already evaluated this contribution in subsubsect. 5.1.1. It gives the terms T_5-T_8 of eq. (51). We showed that only T_5 and T_8 were non-vanishing and lead to the t-channel of quark-antiquark scattering and to the t- and u-channel of quark-quark scattering shown in fig. 7 a) and b). In each of these channels the gluonic propagator cannot be on-mass shell. Therefore the on-shell part of G^{--} does not contribute and we can replace the non-equilibrium propagator G^{--} by the Feynman propagator $G_{\rm F}$.

In subsect. 5.1.1, we derived the mixed terms for qq and $q\bar{q}$ scattering from the exchange graph $\Sigma^{(2)+-}_{\rm E,b)}$ given in eq. (49). We investigate now the question whether it is possible to replace the gluonic non-equilibrium propagators $G^{\mp\mp}$ by the Feynman propagators again. This difference only matters for the s-channel where the gluonic propagator can be on-shell. Therefore we investigate now the mixed term from the s- and t-channel of quark-antiquark scattering. This mixed term is given in the first term of eq. (53) and the contribution of the gluonic propagators reads $G^{--}(X,p+p_1)\,G^{++}(X,p-p_3)+G^{--}(X,p-p_3)\,G^{++}(X,p+p_1)$. Setting $G^{\mp\mp}=G^{(*)}_{\rm F}+G_{\rm n.e.}$, where $G_{\rm n.e.}$ denotes the on-shell non-equilibrium part of the diagonal propagators, and using the fact that the gluon propagator of the t-channel is off-shell, we find

$$
\begin{aligned}
&G^{--}(X,p+p_1)\,G^{++}(X,p-p_3)\\
&+G^{--}(X,p-p_3)\,G^{++}(X,p+p_1)\\
&=[G_{\rm F}(X,p+p_1)+G_{\rm n.e.}(X,p+p_1)]\,{\rm P}\frac{-i}{(p-p_3)^2-m^2}\\
&+{\rm P}\frac{i}{(p-p_3)^2-m^2}\,[G^*_{\rm F}(X,p+p_1)+G_{\rm n.e.}(X,p+p_1)]\\
&=G_{\rm F}(X,p+p_1)\,{\rm P}\frac{-i}{(p-p_3)^2-m^2}\\
&+{\rm P}\frac{i}{(p-p_3)^2-m^2}\,G^*_{\rm F}(X,p+p_1). \qquad (98)
\end{aligned}
$$

Thus the non-equilibrium part of the gluonic propagator of the s-channel does not contribute and one can replace the non-equilibrium propagators by their Feynman counterparts. To summarize, the contributions of $\Sigma^{(2)+-}_{\rm QL,a)}$ and $\Sigma^{(2)+-}_{\rm Eb)}$ to the collision integral read

$$
\begin{aligned}
&J^{(2)\rm loss}_{{\rm coll},q}=\frac{\pi}{E_p}\int\frac{{\rm d}^3p_1}{2E_1(2\pi)^3}\,\frac{{\rm d}^3p_3}{2E_3(2\pi)^3}\,\frac{{\rm d}^3p_4}{2E_4(2\pi)^3}\\
&\times(2\pi)^4\,\delta^{(4)}(p+p_1-p_3-p_4)\\
&\times\left\{\frac{1}{2}\,|\mathcal{M}_{qq\to qq}|^2\;f_q(X,\vec{p})\,f_q(X,\vec{p}_1)\,\bar{f}_q(X,\vec{p}_3)\,\bar{f}_q(X,\vec{p}_4)\right.\\
&\left.+\,|\mathcal{M}_{q\bar{q}\to q\bar{q}}|^2\,f_q(X,\vec{p})\,f_{\bar{q}}(X,\vec{p}_1)\,\bar{f}_q(X,\vec{p}_3)\,\bar{f}_{\bar{q}}(X,\vec{p}_4)\right\}\\
&+\frac{\pi}{E_p}\int\frac{{\rm d}^3p_1}{2E_1(2\pi)^3}\,\frac{{\rm d}^3p_2}{2E_2(2\pi)^3}\,(2\pi)^4\,\delta^{(4)}(p+p_1-p_2)\\
&\times\mathcal{M}^{a)}_{q\bar{q}\to g}\,[\mathcal{M}^{d')}_{q\bar{q}\to g}]^\dagger\,f_q(X,\vec{p})\,f_{\bar{q}}(X,\vec{p}_1)\,\bar{f}_g(X,\vec{p}_2), \qquad (99)
\end{aligned}
$$

where for the quark-quark and quark-antiquark scattering Feynman propagators are used.

As was stated at the beginning of this section, the product $\mathcal{M}^{a)}_{q\bar{q}\to g}\,[\mathcal{M}^{f')}_{q\bar{q}\to g}]^\dagger$ is still missing. Obviously it can only emerge from the self-energy graph $\Sigma^{(2)+-}_{\rm R,a)}$. Since the rainbow and the quark-loop graphs have similar topologies, this product can be derived in an analogous way. In subsubsect. 5.1.2, we showed that $\Sigma^{(2)+-}_{\rm R,a)}$ yields the t- and u-channel of the process $q\bar{q}\to gg$ and the s- and u-channel of the process $qg\to qg$ shown in fig. 7. Due to our choice of masses none of the propagators of these channels can be on-mass shell, *i.e.* only the principal values of the propagators contribute. Therefore it makes no difference if one uses the non-equilibrium or the (temperature independent) Feynman propagators! We emphasize that the self-energy graph $\Sigma^{(2)+-}_{\rm R,a)}$ not only yields the above-mentioned absolute squares of scattering channels but also the "missing" product $\mathcal{M}^{a)}_{q\bar{q}\to g}\,[\mathcal{M}^{f')}_{q\bar{q}\to g}]^\dagger$ without any change of propagators. This result is quite surprising and could not be derived by any "cutting rules".

We comment that also the gluonic propagator is off-shell for the s-channel of the process $q\bar{q}\to gg$. Otherwise it could not decay into two on-shell gluons.

We conclude that only the exchange propagator of the s-channel of $q\bar{q}$ scattering can be on-mass shell, and only in this case the substitution of the non-equilibrium propagator by the Feynman propagator matters.

We summarize the result of this section. Collecting all contributions of the Fock and the two-loop self-energies to the collision integral, the transport equation reads

$$
\begin{aligned}
&2p\partial_X f_q(X,p)=\int\frac{{\rm d}^3p_1}{(2\pi)^3 2E_1}\,\frac{{\rm d}^3p_2}{(2\pi)^3 2E_2}\\
&\times(2\pi)^4\delta^{(4)}(p+p_1-p_2)|\mathcal{M}_{g\to q\bar{q}}|^2\\
&\times[f_g(X,p_2)\bar{f}_{\bar{q}}(X,p_1)\bar{f}_q(X,p)\\
&-\bar{f}_g(X,p_2)f_{\bar{q}}(X,p_1)f_q(X,p)]\\
&+\int{\rm d}\Omega\frac{{\rm d}^3p_1}{(2\pi)^3 2E_1}\,|\vec{v}_p-\vec{v}_1|\,2E_p\,2E_1\\
&\times\left\{\sum_{j=1}^{4}s_j\frac{{\rm d}\sigma_j}{{\rm d}\Omega}\Big|_{qa\to bc}\right.\\
&\times\left.\left[\bar{f}_q(X,\vec{p})\,\bar{f}_a(X,\vec{p}_1)\,f_b(X,\vec{p}_3)\,f_c(X,\vec{p}_4)\right.\right.\\
&\left.\left.-f_q(X,\vec{p})\,f_a(X,\vec{p}_1)\,\bar{f}_b(X,\vec{p}_3)\,\bar{f}_c(X,\vec{p}_4)\right]\right\}, \qquad (100)
\end{aligned}
$$

where j denotes the four processes $j=1...4$ corresponding to $q\bar{q}\to gg$, $qg\to qg$, $qq\to qq$ and $q\bar{q}\to q\bar{q}$. The s_j are symmetry factors $s_1=s_3=1/2$ and $s_2=s_4=1$. This equation is correct up to order g^4m^4.

For the evaluation of the $2\to 2$ cross-sections, the Feynman propagators, *i.e.* the $T=0$ equilibrium propagators were used, while for the evaluation of the process $q\bar{q}\to g$ up to order g^4m^4 the non-equilibrium propagators of eqs. (20) to (23) were used.

One last comment is in order: for this derivation we evaluated the self-energy graphs directly with the help of Feynman rules. We were able to rewrite each self-energy

graph in terms of one or several products of scattering amplitudes. It is not possible to find "cutting rules" from which the same result could be obtained.

Let us now compare our work with results found by other authors. Blaizot and Iancu [15] found a collision term containing the absolute square of a matrix element corresponding to the t-channel of particle-particle scattering, and to the s- and t-channel of particle-antiparticle scattering. The u-channel of particle-particle scattering nor the mixed terms between the channels are included. For the evaluation of the scattering amplitudes the *equilibrium retarded* propagator is used and not the causal propagator as we have.

Baier *et al.* [28] study the production of thermal dileptons in a hot pion gas, examining the two-loop diagrams that can occur within the theory. In their approach, these graphs are subdivided as giving rise to real and virtual processes, and in doing so, the exchanged meson is represented accordingly by its principal or thermal parts, respectively.

6 n ⟶ m processes

Up to this point, we have made a semiclassical expansion that involves keeping only the leading term in expanding the exponential in eq. (19) (here the factor $\hbar$ has been set to one.) In addition, we have examined sets of diagrams organized according to the number of interaction lines, *i.e.* according to the coupling strength. We have found that all generic types of graphs are required in order to build up the cross-sections that ultimately occur in a Boltzmann-like equation. However, at the level of two exchanged gluons, we are already faced with five types of graphs, and this number increases rapidly with the number of exchanged gluons. One possible simplifying assumption is the additional imposition of an expansion in the inverse number of colors. According to such a criterion, the ladder, the rainbow and the cloud diagrams are leading, since their color factors for one color group are of order $O(N_c^2)$, while for the quark-loop diagram it goes as N_c and for the exchange diagram only as N_c^0 (see appendix C).

Since the ladder and the rainbow diagrams lead to cross-sections involving gluons while the quark-loop diagram leads to elastic quark-(anti)quark cross-sections, one can conclude that the quark degrees of freedom are suppressed in comparison with the gluon degrees of freedom. This is in agreement with the results of an evaluation of the quark-quark scattering amplitude within this model [17], in which the quark degrees of freedom are neglected, however due to kinematical reasons. Although the ladder and the rainbow diagrams are both of order $O(N_c^2)$, the ratio of their color factors for one color group is not one, but

$$\frac{F_{\mathrm{R}}}{F_{\mathrm{L}}} = \frac{C_{\mathrm{F}}}{C_{\mathrm{A}}}, \tag{101}$$

which is $4/9 \approx 1/2$ for $N_c = 3$. Since in the rainbow diagram the second gluon couples at the quark-line while in the ladder diagram it couples at the first gluon, two quark-quark-gluon vertices are suppressed by a factor 4/9 per color group in comparison with two 3-gluon vertices. Thus, there is no *strict* ordering of the gluon graphs according to a single class of diagrams, in an expansion in $1/N_c$. Although the ladder graphs and the processes that they lead to appear largest, one should note that the symmetry factors of the other graphs compensate for this. A numerical study is essential to determine the actual order of magnitude of each graph.

Note that an expansion in color also incorporates the coupling strength. Assuming that $g \sim 1/N_c$, we find that the Fock term $\sim g^2 N_c^2$ and the ladder diagram $\sim g^4 N_c^4$ are of the same order.

Of the self-energy diagrams of order $O(g^{2n})$, the ladder diagram, the rainbow diagram and all possible mixtures between these two are leading in an expansion in $1/N_c$. On evaluation, these diagrams lead to the scattering process $q\bar{q} \to ng$ and all possible crossed processes, such as $q\bar{q}g \to (n-1)g$, $qg \to q(n-1)g$, ... in which at least two partons occur both in the initial and final states. In addition to this, they lead to corrections of order $O(g^{2n})$ to lower-order processes. The Boltzmann equation for quarks then reads

$$\begin{aligned}
&2p\partial_X f_q(X,\vec{p}) = \int \frac{\mathrm{d}^3k}{(2\pi)^3 2E_k}\frac{\mathrm{d}^3p_1}{(2\pi)^3 2E_1} \\
&\times(2\pi)^4\delta^{(4)}(p+k-p_1)|\mathcal{M}_{q\bar{q}\to g}|^2 \\
&\times\Big[\bar{f}_q(X,\vec{p})\bar{f}_{\bar{q}}(X,\vec{k})f_g(X,\vec{p}_1) \\
&-f_q(X,\vec{p})f_{\bar{q}}(X,\vec{k})\bar{f}_g(X,\vec{p}_1)\Big] \\
&+\sum_{m,n=1}^{\infty}\int \frac{\mathrm{d}^3k}{(2\pi)^3 2E_k}\frac{\mathrm{d}^3p_1}{(2\pi)^3 2E_1}\cdots\frac{\mathrm{d}^3p_{m+n}}{(2\pi)^3 2E_{m+n}}(2\pi)^4 \\
&\times\Big\{\delta^{(4)}(p+k+p_1+...+p_{m-1}-p_m-...-p_{m+n}) \\
&\times s_{m-1}s_{n+1}\ |\mathcal{M}(q\bar{q}\,(m-1)g\to(n+1)g)|^2 \\
&\times\Big[\bar{f}_q(\vec{p})\bar{f}_{\bar{q}}(\vec{k})\bar{f}_g(\vec{p}_1)...\bar{f}_g(\vec{p}_{m-1})f_g(\vec{p}_m)...f_g(\vec{p}_{m+n}) \\
&-f_q(\vec{p})f_{\bar{q}}(\vec{k})f_g(\vec{p}_1)...f_g(\vec{p}_{m-1})\bar{f}_g(\vec{p}_m)...\bar{f}_g(\vec{p}_{m+n})\Big] \\
&+\delta^{(4)}(p+p_1+...+p_m-k-p_{m+1}-... \\
&-p_{m+n})s_m s_n\ |\mathcal{M}(q\,mg\to q\,ng)|^2 \\
&\times\Big[\bar{f}_q(\vec{p})\bar{f}_g(\vec{p}_1)...\bar{f}_g(\vec{p}_m)f_q(\vec{k})f_g(\vec{p}_{m+1})...f_g(\vec{p}_{m+n}) \\
&-f_q(\vec{p})f_g(\vec{p}_1)...f_g(\vec{p}_m)\bar{f}_q(\vec{k})\bar{f}_g(\vec{p}_{m+1})...\bar{f}_g(\vec{p}_{m+n})\Big]\Big\}
\end{aligned} \tag{102}$$

with the symmetry factors $s_n = 1/n!$.

7 Pinch singularities

When dealing with transport theory, and in particular when applying the quasiparticle assumption to processes of higher order, it becomes mandatory to examine another

possible problem which can arise, the issue of so-called pinch singularities. To elucidate this, let us look again at the quark-loop self-energy diagrams shown in fig. 6. We can write the sum of these four self-energy graphs as

$$\begin{aligned}&\Sigma^{(2)+-}_{\rm QL}(X,p) \equiv \Sigma^{(2)+-}_{\rm QL,a)}(X,p) + \Sigma^{(2)+-}_{\rm QL,b)}(X,p)\\ &+\Sigma^{(2)+-}_{\rm QL,c)}(X,p) + \Sigma^{(2)+-}_{\rm QL,d)}(X,p) =\\ &ig^2m^2\int\frac{{\rm d}^4k}{(2\pi)^4}\,iS^{+-}(X,p-k)\,iF^{+-}_{\rm QL}(X,k)\end{aligned} \tag{103}$$

with

$$\begin{aligned}F^{+-}_{\rm QL}(X,k) \equiv\ & G^{++}(X,k)\,\Pi^{+-}(X,k)\,G^{--}(X,k)\\ &+G^{++}(X,k)\,\Pi^{++}(X,k)\,G^{+-}(X,k)\\ &+G^{+-}(X,k)\,\Pi^{--}(X,k)\,G^{--}(X,k)\\ &+G^{+-}(X,k)\,\Pi^{-+}(X,k)\,G^{+-}(X,k)\,,\end{aligned} \tag{104}$$

where Π^{ij} is defined in eq. (72) and all color factors are suppressed for simplicity.

We see that in eq. (104) each term contains two gluonic propagators with the same argument. Since the off-diagonal propagators are on-shell and also the diagonal propagator contain on-shell parts, seen in the δ-functions that are present, we obtain for each term a product of two δ-functions, which is clearly divergent.

This is a manifestation of so-called pinch singularities. The etymology is made evident if we express $F^{+-}_{\rm QL}$ in terms of the retarded and advanced components given in eqs. (B.4), (B.5), (B.11) and (B.12):

$$\begin{aligned}F^{+-}_{\rm QL}(X,k) \equiv\ & G^{\rm R}(X,k)\,\Pi^{\rm R}(X,k)\,G^{+-}(X,k)\\ &+G^{+-}(X,k)\,\Pi^{\rm A}(X,k)\,G^{\rm A}(X,k)\\ &-G^{\rm R}(X,k)\,\Pi^{+-}(X,k)\,G^{\rm A}(X,k).\end{aligned} \tag{105}$$

In the last term the product

$$G^{\rm R}(X,k)\,G^{\rm A}(X,k) = \frac{1}{k^2-m^2+i\epsilon}\,\frac{1}{k^2-m^2-i\epsilon} \tag{106}$$

has a pinch singularity, since an integration contour running along the real k_0 axis is "pinched" between the two poles for $\epsilon\to 0$. For the rainbow and ladder self-energy graphs of fig. 6, the situation is similar as for the quark-loop graph: each graph contains two propagators with the same argument. Therefore pinch singularities may occur in these terms, too.

In *equilibrium*, however, studies over the last decade show that pinch singularities vanish in the calculations of physical quantities [29,30] in a well-defined theory (such as thermal field theory). Since in the literature, there are only a few examples for a few cases, we indicate explicitly in appendix D how the pinch singularities are canceled for the self-energies that are required in our model, see fig. 6, when considered in equilibrium. Unfortunately, these calculations cannot be generalized for the case of non-equilibrium since the derivation depends on the KMS relation, which is only valid in equilibrium.

To conclude this section, we mention several results in the literature: Dadić developed two mechanisms for the elimination of pinch singularities in non-equilibrium [31]. The first one is based on the vanishing of phase space at the singular point, and it can be applied, *e.g.*, to QED with massive electrons and massless photons. This however does not apply to our theory, since we have massless quarks and massive gluons. Greiner and Leupold [32] have showed that the pinch singularities are due to the infinite duration time of the interaction and can be regulated by a finite duration time. Bedaque [33] has argued that pinch singularities do not appear in non-equilibrium if the interaction is switched on at a finite time (should the fields have interacted since $t=-\infty$, they should have attained equilibrium by any finite time).

8 The constraint equation

So far we have treated only the transport equation (28) as an isolated equation. As we have seen, this in itself has a complexity in deriving an extended Boltzmann equation. The main assumption that has been made is the quasiparticle approximation, and this has been inserted into every level of calculation of the self-energy. In principle, however, the transport equation does not stand alone, but must be solved simultaneously with the constraint equation, which in practice must be newly evaluated for each additional term in the expansion (here in the coupling constant and of the self-energy) that has been used. In sect. 3, we demonstrated explicitly that the constraint equation gives rise to the quasiparticle approximation for free streaming. Here this corresponds to the Hartree approximation for the self-energy. In general, however, this is not so. We thus take a closer look at the constraint equation (29). Using the relations (B.2),(B.3) and (B.9), we can rewrite the constraint equation in a simpler form as

$$\begin{aligned}&\left[p^2-M^2+\Re\Pi^{--}(X,p)\right]D^{-+}(X,p) =\\ &\quad\Pi^{-+}(X,p)\,\Re D^{--}(X,p).\end{aligned} \tag{107}$$

With the aid of eqs. (B.2), (B.4), (B.5), (B.26) and (B.27), we can express the real part of D^{--} as

$$\begin{aligned}&2\Re D^{--}(X,p) = D^{--}(X,p) - D^{++}(X,p) =\\ &\quad D^{\rm R}(X,p) + D^{\rm A}(X,p) =\\ &\frac{1}{p^2-M^2+\Pi^{\rm R}(X,p)} + \frac{1}{p^2-M^2+\Pi^{\rm A}(X,p)}.\end{aligned} \tag{108}$$

Using eqs. (B.10) to (B.12), one finds

$$\Re\Pi^{\rm R}(X,p) = \Re\Pi^{\rm A}(X,p) = \Re\Pi^{--}(X,p)\,, \tag{109}$$

$$\Im\Pi^{\rm R}(X,p) = -\Im\Pi^{\rm A}(X,p) = p_0\,\Gamma(X,p)\,, \tag{110}$$

where the width Γ is defined as

$$\Gamma(X,p) = \frac{i}{2p_0}(\Pi^{+-}-\Pi^{-+}). \tag{111}$$

Inserting eqs. (109) and (110) into eq. (108) leads to

$$\Re D^{--}(X,p) = \frac{p^2 - M^2 + \Re\Pi^{--}(X,p)}{\left[p^2 - M^2 + \Re\Pi^{--}(X,p)\right]^2 + \left[p_0\,\Gamma(X,p)\right]^2}. \tag{112}$$

Substituting p with $-p$ in eq. (107) yields the relation

$$\left[p^2 - M^2 + \Re\Pi^{--}(X,p)\right] D^{+-}(X,p) = \Pi^{+-}(X,p)\,\Re D^{--}(X,p). \tag{113}$$

Subtracting (107) from (113) gives

$$\left[p^2 - M^2 + \Re\Pi^{--}(X,p)\right] \mathcal{A}(X,p) = 2p_0\,\Gamma(X,p)\,\frac{p^2 - M^2 + \Re\Pi^{--}(X,p)}{\left[p^2 - M^2 + \Re\Pi^{--}(X,p)\right]^2 + \left[p_0\,\Gamma(X,p)\right]^2}, \tag{114}$$

where the spectral density $\mathcal{A}$ is defined through the combination

$$\mathcal{A}(X,p) = iD^{+-}(X,p) - iD^{-+}(X,p). \tag{115}$$

For $p^2 - M^2 + \Re\Pi^{--}(X,p) \neq 0$, eq. (114) gives

$$\mathcal{A}(X,p) = \frac{2p_0\,\Gamma(X,p)}{\left[p^2 - M^2 + \Re\Pi^{--}(X,p)\right]^2 + \left[p_0\,\Gamma(X,p)\right]^2}. \tag{116}$$

If $\mathcal{A}$ is calculated, one can immediately find expressions for the off-diagonal Green functions via

$$iD^{-+}(X,p) = \Theta(p_0)\,\mathcal{A}(X,p)\,f_a(X,p) - \Theta(-p_0)\,\mathcal{A}(X,p)\,\bar{f}_{\bar{a}}(X,-p)\,, \tag{117}$$

$$iD^{+-}(X,p) = \Theta(p_0)\,\mathcal{A}(X,p)\,\bar{f}_a(X,p) - \Theta(-p_0)\,\mathcal{A}(X,p)\,f_{\bar{a}}(X,-p)\,, \tag{118}$$

and subsequently for the diagonal Green functions with the help of eqs. (22) and (23). In the limit of vanishing self-energies (and therefore vanishing width Γ) $\mathcal{A}$ simplifies to

$$\mathcal{A}(X,p) \longrightarrow 2\pi\delta(p^2 - M^2)\,\mathrm{sign}(p_0) \tag{119}$$

and for the Green functions one regains the quasiparticle approximation eqs. (20) to (23) as it should be.

One thus finds the situation that higher-order corrections to the transport equation should, strictly speaking, be evaluated with propagators that contain a finite width Γ. This has both advantages and disadvantages. The main advantage is that no pinch singularities can possibly occur with the use of a finite width by definition (see also ref. [34]). Thus, one may definitively state that non-equilibrium theory is non-singular; any apparent singularities are a result of using an inconsistent approximation and these may be removed by the introduction of a cutoff related to a width.

The disadvantages of using a finite width are manifold: Firstly the presence of a finite width automatically admits all possible processes: for example, the first exchange and quark-loop diagrams led to a sum of eight terms, eq. (51). These in turn led to two possible types of scattering processes that were admissible, with the restriction being directly due to the quasiparticle assumption. In the presence of a finite width, all eight terms would be non-vanishing. In this sense, the theory is expanded well over the Boltzmann approach. Furthermore, an additional complexity arises. The transition from Green functions to the more physical quantities, the distribution functions, in terms of which the Boltzmann equation is expressed, no longer becomes possible. Thus the evaluation of physical entities becomes more distanced from our knowledge of the Boltzmann equation. It is our point of view that research in both directions is interesting. While it is more easily conceivable to do physics in extending the Boltzmann equation, it is equally necessary to attempt to solve the exact equations, and determine the difference between these two approaches. From an analytic point of view, it is not simple to extract this difference. Rather numerical calculations should prove interesting and insightful.

In the literature [13], the assumption of a finite width is made and introduced into transport equations. At this point, however, all connection with field theory becomes obscure: it is now essential to introduce a "test-particle ansatz", as the spectral distribution is altered, and a direct connection to diagrams is no longer evident.

9 Summary and conclusions

In this paper, we have detailed the calculation of the transport and constraint equations for a theory of scalar quarks and gluons. Special care has been taken in particular in understanding how the transport equation, taken on its own, leads to a Boltzmann-like equation when considered in the quasiparticle approximation. This calculation goes beyond those previously mentioned in the literature, in that all the graphs that occur are analyzed in their full complexity. Through this analysis, it is evident which role they play: certain graphs give rise to the expected cross-sections, while others serve to renormalize lower-order diagrams to the same order in the coupling constant. It is furthermore an interesting result that the diagrammatics of this theory that favor only gluon ladder graphs in qq scattering is not simply reflected here. In a $1/N_c$ approximation, all gluonic processes dominate over quark loop processes, but gluon ladders per se are not singled out. This result can be generalized to higher orders.

Several problems emerged in the calculation of the transport equation: firstly it is not independent of the constraint equation, and secondly several terms within the quasiparticle approximation appear individually to be singular. We have thus devoted a section to the discussion of the constraint equation pointing out the advantages and disadvantages of introducing a width. The issue of pinch singularities on its own has also been discussed in detail. In particular, we have demonstrated that the singularities in a series of graphs vanish, at least when considered in equilibrium. An exact proof in non-equilibrium has however not been found.

One of us (D.S.I.) wishes to thank J. Hüfner, M. Schmidt, C. Greiner and S. Leupold for stimulating discussions.

Appendix A. Real-time thermal field theory

In this appendix, we briefly review the real-time formalism of thermal field theory (see *e.g.* [35,36,23]). The real-time contour goes from $-\tau$ to $+\tau$ on the real axis, then drops vertically down to $+\tau - i\sigma$, runs parallel to the real axis back to $-\tau - i\sigma$ and finally down to $-\tau - i\beta$. Here the parameter σ takes a value between 0 and β. One assumes that in the limit $\tau \to \infty$ the vertical segments of the contour C decouple in the path integral and do not contribute to Green functions with time arguments on the horizontal segments. For simplicity, the spatial coordinates are suppressed in this appendix. Writing the fields on the upper and the lower horizontal segments as functions of real times, $\hat{\phi}_-(t) = \hat{\phi}(t)$ and $\hat{\phi}_+(t) = \hat{\phi}(t - i\sigma)$, respectively, the generating functional for the Green functions reads as

$$Z[J_+, J_-] = Z[0,0] \left\langle T_C \exp\left\{ i \int_{-\infty}^{\infty} \mathrm{d}t\, \hat{\phi}_s J_s \right\} \right\rangle , \quad \text{(A.1)}$$

where the sign index s runs over $\{-,+\}$ and $J_-(t)$ is defined to be the source on the upper segment and $J_+(t) = -J(t - i\sigma)$ the source on the lower one. The minus sign in the latter absorbs the minus sign from the opposite direction of the lower contour. Note, that in our notation the "$-$" sign is associated with the upper branch as in [20] and in contrast to [36]. In the '80s, the "$-$" fields were termed physical fields according to the idea that physical observables would be expressible in terms of Green functions with only "$-$" fields on the external legs. The "$+$" fields were consistently called ghost fields. This is not a valid supposition. As a simple example, the mass term Π^{R} is made up of both Π^{--} and Π^{-+}, see eq. (B.11). There are also other interesting physical quantities with "$+$" fields on their external legs, see, *e.g.*, the collision term of eq. (16).

Differentiation with respect to $J_-(t)$ and $J_+(t)$ then gives the real-time Green functions

$$G_\sigma^{s_1 \cdots s_N}(t_1, \ldots t_N) := \left. \frac{\delta_{iJ_{s_1}(t_1)} \ldots \delta_{iJ_{s_N}(t_N)}\, Z[J_-, J_+]}{Z[J_-, J_+]} \right|_{J_-=0, J_+=0} . \quad \text{(A.2)}$$

The contour ordering T_C implies that this real-time Green function is the thermal average of a product of field operators where the ordering is such that the "$-$" fields are time-ordered and put on the right-hand side and the "$+$" fields are anti-time-ordered and put on the left-hand side. Performing a Fourier transform

$$G_\sigma^{s_1 \cdots s_N}(\omega_1, \ldots, \omega_N) := \int \mathrm{d}t_1 \ldots \mathrm{d}t_N \, \exp\left\{ i \sum_i \omega_i t_i \right\} G^\sigma_{s_1 \ldots s_N}(t_1, \ldots, t_N) \quad \text{(A.3)}$$

yields the relation between Green functions with different values of σ,

$$G_\sigma^{s_1 \cdots s_N}(\omega_1, \ldots, \omega_N) = \exp\left\{ - \sum_{i|s_i=+} \sigma\, \omega_i \right\} G^{s_1 \ldots s_N}_{\sigma=0}(\omega_1, \ldots, \omega_N). \quad \text{(A.4)}$$

Note that the value $\sigma = 0$ corresponds to a closed time path (CTP) or Schwinger-Keldysh formalism, see fig. 3, while $\sigma = \beta/2$ corresponds to the choice for thermo field dynamics. From eq. (A.2) one obtains the real-time propagators as

$$\begin{aligned} iD_\sigma^{--}(t - t') &= \langle T \hat{\phi}(t) \hat{\phi}(t') \rangle , \\ iD_\sigma^{++}(t - t') &= \langle \tilde{T} \hat{\phi}(t - i\sigma) \hat{\phi}(t' - i\sigma) \rangle , \\ iD_\sigma^{+-}(t - t') &= \langle \hat{\phi}(t - i\sigma) \hat{\phi}(t') \rangle , \\ iD_\sigma^{-+}(t - t') &= \langle \hat{\phi}(t' - i\sigma) \hat{\phi}(t) \rangle . \end{aligned} \quad \text{(A.5)}$$

These four propagators can be written in a compact matrix form as

$$\underline{D}_\sigma = \begin{pmatrix} D_\sigma^{--} & D_\sigma^{-+} \\ D_\sigma^{+-} & D_\sigma^{++} \end{pmatrix}. \quad \text{(A.6)}$$

Performing a Fourier transform yields

$$i\underline{D}(\omega) = \begin{pmatrix} iD_{\mathrm{F}}(\omega) & 0 \\ 0 & iD_{\mathrm{F}}^*(\omega) \end{pmatrix} + 2\pi\delta(\omega^2 - E^2) \times \begin{pmatrix} n(|\omega|) & e^{\sigma\omega}[\Theta(-\omega) + n(|\omega|)] \\ e^{-\sigma\omega}[\Theta(\omega) + n(|\omega|)] & n(|\omega|) \end{pmatrix} , \quad \text{(A.7)}$$

where iD_{F} is the $T = 0$ Feynman propagator given by

$$iD_{\mathrm{F}}(\omega) = \frac{i}{p^2 - m^2 + i\epsilon} \quad \text{(A.8)}$$

and $n(\omega)$ is the Bose distribution defined by

$$n(\omega) = \frac{1}{e^{\beta\,\omega} - 1}. \quad \text{(A.9)}$$

The real-time Feynman rules are much the same as in zero-temperature field theory. The only difference is, that to each vertex a sign factor $s = -, +$ is assigned. For Green functions, the external vertices are fixed, and all internal vertices are summed over (which multiplies the number of graphs, see, *e.g.*, figs. 4 and 6). A vertex with $s = -$ corresponds to a factor $-igm$, while a vertex with $s = +$ corresponds to a factor $+igm$. A line connecting a vertex s with a vertex s' corresponds to a propagator $D_{ss'}$ given in eq. (A.5).

An example for a scattering amplitude is shown in fig. 8. The external vertices are fixed to be $s = -$, while the internal vertices can be either $-$ or $+$ and one has to draw all possibilities. The complex conjugate of such an amplitude (*in position space*) is obtained by interchanging all "$-$" vertices with "$+$" vertices and vice versa in the original amplitude.

The CTP formalism ($\sigma = 0$) is now easily generalized for non-equilibrium processes by replacing the equilibrium, real-time thermal propagators defined in eq. (A.2) by the non-equilibrium propagators given in eqs. (10) and (11).

Appendix B. Green functions, transport and constraint equations

In this appendix, we give a brief guideline for the derivation of the transport and constraint equations, eqs. (13) and (14) and list all important properties of the Green functions.

The Schwinger-Keldysh Green functions defined in eqs. (10) and (11) can be collected in a matrix as

$$\underline{D} = \begin{pmatrix} D^{--} & D^{-+} \\ D^{+-} & D^{++} \end{pmatrix}, \tag{B.1}$$

using the generic notation already introduced in sect. 3. From the definition of the Green functions, it follows that

$$\left[iD^{--}(x,y)\right]^\dagger = iD^{++}(x,y), \tag{B.2}$$

while $iD^{\pm\mp}$ is Hermitian (*e.g.*, $[iD^{-+}(x,y)]^\dagger = iD^{+-}(x,y)$), and the relation

$$D^{--}(x,y)+D^{++}(x,y)=D^{-+}(x,y)+D^{+-}(x,y), \tag{B.3}$$

showing that the four components D^{ij} are not independent. We define the retarded and advanced Green functions in the standard way as

$$\begin{aligned} D^{\mathrm{R}}(x,y) :=& \ \Theta(x_0-y_0)[D^{+-}(x,y)-D^{-+}(x,y)] \\ =& \ D^{--}(x,y)-D^{-+}(x,y) \\ =& \ D^{+-}(x,y)-D^{++}(x,y) \end{aligned} \tag{B.4}$$

$$\begin{aligned} D^{\mathrm{A}}(x,y) :=& -\Theta(y_0-x_0)[D^{+-}(x,y)-D^{-+}(x,y)] \\ =& \ D^{--}(x,y)-D^{+-}(x,y) \\ =& \ D^{-+}(x,y)-D^{++}(x,y). \end{aligned} \tag{B.5}$$

The equations of motion that the Green functions satisfy are

$$\begin{aligned} (\Box_x + M^2)\underline{D}(x,y) =& -\underline{\sigma}_z\delta^{(4)}(x-y) \\ &+\int \mathrm{d}^4z\, \underline{\sigma}_z\, \underline{\Pi}(x,z)\underline{D}(z,y), \end{aligned} \tag{B.6}$$

given in terms of the irreducible proper self-energy

$$\underline{\Pi} = \begin{pmatrix} \Pi^{--} & \Pi^{-+} \\ \Pi^{+-} & \Pi^{++} \end{pmatrix} \tag{B.7}$$

and

$$\underline{\sigma}_z = \begin{pmatrix} 1 & 0 \\ 0 & -1 \end{pmatrix}. \tag{B.8}$$

In eq. (B.6), M is the free bosonic parton mass.

The four components of the self-energy are also not independent. From their definition, the relation

$$\Pi^{--}(x,y)+\Pi^{++}(x,y)=-(\Pi^{+-}(x,y)+\Pi^{-+}(x,y)) \tag{B.9}$$

can be seen to hold. The off-diagonal components are again Hermitian, while the diagonal ones fulfill

$$\left[i\Pi^{--}(x,y)\right]^\dagger = i\Pi^{++}(x,y). \tag{B.10}$$

The retarded and advanced self-energies are defined to be

$$\Pi^{\mathrm{R}}(x,y) = \Pi^{--}(x,y) + \Pi^{-+}(x,y)\,, \tag{B.11}$$

$$\Pi^{\mathrm{A}}(x,y) = \Pi^{--}(x,y) + \Pi^{+-}(x,y)\,. \tag{B.12}$$

We now consider specifically the equation of motion for D^{-+}. This reads

$$\begin{aligned} (\Box_x + M^2)D^{-+}(x,y) =& \int \mathrm{d}^4z\{\Pi^{--}(x,z)D^{-+}(z,y) \\ &+\Pi^{-+}(x,z)D^{++}(z,y)\} = \int \mathrm{d}^4z\{\Pi^{\mathrm{A}}(x,z)D^{-+}(z,y) \\ &-\Pi^{+-}(x,z)D^{-+}(z,y) + \Pi^{-+}(x,z)D^{+-}(z,y) \\ &-\Pi^{-+}(x,z)D^{\mathrm{R}}(z,y)\}\,, \end{aligned} \tag{B.13}$$

while the conjugate equation is

$$\begin{aligned} (\Box_y + M^2)D^{-+}(x,y) =& -\int \mathrm{d}^4z\{D^{-+}(x,z)\Pi^{++}(z,y) \\ &+D^{--}(x,z)\Pi^{-+}(z,y)\} = \int \mathrm{d}^4z\{D^{-+}(x,z)\Pi^{\mathrm{A}}(z,y) \\ &-D^{\mathrm{R}}(x,z)\Pi^{-+}(z,y)\}. \end{aligned} \tag{B.14}$$

Now a Wigner transformation of both equations is performed to yield

$$\begin{aligned} &\left[\frac{1}{4}\Box_X - ip\partial_X - p^2 + M^2\right] D^{-+}(X,p) = \\ &\Pi^{\mathrm{A}}(X,p)\hat{\Lambda}D^{-+}(X,p) - \Pi^{+-}(X,p)\hat{\Lambda}D^{-+}(X,p) \\ &+\Pi^{-+}(X,p)\hat{\Lambda}D^{+-}(X,p) - \Pi^{-+}(X,p)\hat{\Lambda}D^{\mathrm{R}}(X,p) \end{aligned} \tag{B.15}$$

and

$$\begin{aligned} &\left[\frac{1}{4}\Box_X + ip\partial_X - p^2 + M^2\right] D^{-+}(X,p) = \\ &D^{-+}(X,p)\hat{\Lambda}\Pi^{\mathrm{A}}(X,p) - D^{\mathrm{R}}(X,p)\hat{\Lambda}\Pi^{-+}(X,p), \end{aligned} \tag{B.16}$$

with the differential operator

$$\hat{\Lambda} := \exp\left\{\frac{-i}{2}\left(\overleftarrow{\partial}_X\overrightarrow{\partial}_p - \overleftarrow{\partial}_p\overrightarrow{\partial}_X\right)\right\}. \tag{B.17}$$

Subtracting eq. (B.15) from eq. (B.16) gives the so-called transport equation,

$$-2ip\partial_X D^{-+}(X,p) = I_-, \tag{B.18}$$

while adding them yields the so-called constraint equation,

$$\left(\frac{1}{2}\Box_X - 2p^2 + 2M^2\right) D^{-+}(X,p) = I_+, \tag{B.19}$$

that were quoted as eqs. (13) and (14), and $I_\mp$ is as given in eqs. (15) to (18).

Here and throughout this paper, we work with the Green functions D^{ij} $(i,j=-,+)$ since they are needed to calculate properties like the self-energy in a diagrammatic expansion. As already mentioned, these four components of $\underline{D}$ given in eq. (B.1) are not independent of each other.

$$\left[\frac{1}{4}\Box_X - ip\partial_X - p^2 + M^2\right]\begin{pmatrix} 0 & D^{\mathrm{A}}(X,p) \\ D^{\mathrm{R}}(X,p) & F(X,p)\end{pmatrix} = \begin{pmatrix} 0 & \Pi^{\mathrm{A}}(X,p)\hat{\Lambda}D^{\mathrm{A}}(X,p) - 1 \\ \Pi^{\mathrm{R}}(X,p)\hat{\Lambda}D^{\mathrm{R}}(X,p) - 1 & \Omega(X,p)\hat{\Lambda}D^{\mathrm{A}}(X,p) + \Pi^{\mathrm{R}}(X,p)\hat{\Lambda}F(X,p)\end{pmatrix}. \tag{B.25}$$

Therefore it is possible to transform this matrix that at least one component vanishes. One possible choice is

$$\underline{D}' = U^{-1}\,\underline{D}\,U = \begin{pmatrix} 0 & D^{\mathrm{A}} \\ D^{\mathrm{R}} & F\end{pmatrix} \tag{B.20}$$

with the transformation matrix

$$U = \frac{1}{\sqrt{2}}\begin{pmatrix} 1 & 1 \\ -1 & 1\end{pmatrix}. \tag{B.21}$$

D^{R} and D^{A} are given in eqs. (B.4) and (B.5), respectively, and F is defined as $F = D^{--} + D^{++}$. The same transformation gives for the self-energy

$$\underline{\Pi}' = U^{-1}\,\underline{\Pi}\,U = \begin{pmatrix} \Omega & \Pi^{\mathrm{R}} \\ \Pi^{\mathrm{A}} & 0\end{pmatrix}, \tag{B.22}$$

where Π^{R} and Π^{A} are defined in eqs. (B.11) and (B.12), respectively, and Ω is given as $\Omega = \Pi^{--} + \Pi^{++}$. The equation of motion (B.6) transforms to

$$(\Box_x + M^2)\underline{D}'(x,y) = -\underline{\sigma}_x\delta^{(4)}(x-y) + \int \mathrm{d}^4 z\,\underline{\sigma}_x\,\underline{\Pi}'(x,z)\underline{D}'(z,y), \tag{B.23}$$

with

$$\underline{\sigma}_x = \begin{pmatrix} 0 & 1 \\ 1 & 0\end{pmatrix}. \tag{B.24}$$

Performing a Wigner transformation as above gives

see eq. (B.25) *above*

In a semiclassical expansion $\hat{\Lambda} = 1$ and the derivatives with respect to X in the bracket on the left hand side are neglected. Then the equation for D^{R} can be solved easily to yield

$$D^{\mathrm{R}}(X,p) = \frac{1}{p^2 - M^2 + \Pi^{\mathrm{R}}(X,p)}. \tag{B.26}$$

Similarly, one finds

$$D^{\mathrm{A}}(X,p) = \frac{1}{p^2 - M^2 + \Pi^{\mathrm{A}}(X,p)}, \tag{B.27}$$

which is just the Hermitian of eq. (B.26) and contains therefore no additional information. In sect. 8, these expressions for D^{R} and D^{A} are used.

Appendix C. Color factors

We now deal with the color factors which were neglected so far. We calculate them for *one* $SU(N)$ color group. The overall color factor for both color groups is then obtained by squaring it.

The matrices $(t^a)_{ij}$ are the matrices of the color group in the representation of the quarks, while $(T^a)_{bc} = -if_{abc}$ are the color matrices in the adjoint representation and f_{abc} are the structure constants of the color group, see eq. (2). The t^a's are normalized to

$$\mathrm{tr}(t^a t^b) = \frac{1}{2}\delta_{ab}. \tag{C.1}$$

The "square" of the generator in some representation must be proportional to the unit operator (Schur's Lemma). Therefore

$$(t^a)_{ij}(t^a)_{jk} = C_{\mathrm{F}}\delta_{ik} \tag{C.2}$$

and

$$T^a_{bd}T^a_{dc} = f_{bad}f_{cad} = C_{\mathrm{A}}\delta_{bc}, \tag{C.3}$$

where the numbers C_{F} and C_{A} are the Casimir operators of the fundamental and adjoint representation, respectively. They take the values (see for example [37])

$$C_{\mathrm{F}} = \frac{N_c^2 - 1}{2N_c} \tag{C.4}$$

and

$$C_{\mathrm{A}} = N_c. \tag{C.5}$$

Consider now the quark self-energies that were evaluated in sect. 5.1. Let i denote the external parton color index. It is therefore not to be summed over. The color factor for the rainbow graph is

$$F_{\mathrm{R}} = t^b_{ij}t^a_{jk}t^a_{kl}t^b_{li} = C_{\mathrm{F}}^2\delta_{ii} = \frac{(N_c^2-1)^2}{4N_c^2}\delta_{ii}. \tag{C.6}$$

For the ladder graph, one finds

$$F_{\mathrm{L}} = (-if_{abc})(-if_{cbd})t^a_{ij}t^d_{ji} = C_{\mathrm{A}}\delta_{ad}t^a_{ij}t^d_{ji} = C_{\mathrm{A}}C_{\mathrm{F}}\delta_{ii} = \frac{N_c^2-1}{2}\delta_{ii}. \tag{C.7}$$

For the cloud graph, one obtains

$$F_{\mathrm{C}} = (-if_{acb})t^a_{ij}t^b_{jk}t^c_{ki} = -\frac{N_c^2-1}{4}\delta_{ii}, \tag{C.8}$$

where the relation (see for example [37])

$$-if_{abc}t^a t^b = \frac{C_{\mathrm{A}}}{2}t^c \tag{C.9}$$

has been used. The color factor for the exchange graph is

$$F_{\rm E} = t^a_{ij} t^b_{jk} t^a_{kl} t^b_{li} = -\frac{N_c^2-1}{4N_c^2}\delta_{ii}, \qquad \text{(C.10)}$$

where the relation [37]

$$t^a t^b t^a = \frac{-1}{2N_c} t^b \qquad \text{(C.11)}$$

has been used. Finally, for the quark-loop graph the color factor is given by

$$F_{\rm QL} = t^a_{ij} t^b_{ji} {\rm tr}(t^a t^b) = \frac{N_c^2-1}{4N_c}\delta_{ii}. \qquad \text{(C.12)}$$

In an expansion in $1/N_c$, some of the self-energy diagrams are subleading. For details see sect. 6.

Appendix D. Cancellation of pinch singularities in equilibrium

In this appendix, we show explicitly, that for our cases the pinch singularities vanish in equilibrium. For this purpose it is helpful to use following relations:

$$\Pi^{--}(p) = -\Pi^{++}(p)^*\,, \qquad \text{(D.1)}$$

$$\Im\Pi^{--}(p) = \frac{i}{2}\left[\Pi^{-+}(p) + \Pi^{+-}(p)\right], \qquad \text{(D.2)}$$

$$\Pi^{+-}(p) = e^{\beta p_0}\,\Pi^{-+}(p)\,. \qquad \text{(D.3)}$$

The first two are valid in general while the last one, the so-called Kubo-Martin-Schwinger (KMS) relation, holds only in equilibrium. We start with the sum of the four quark-loop graphs shown in fig. 6 QL a) to QL d). With the help of these relations $F^{+-}_{\rm QL}$ defined in eq. (104) can be written as

$$\begin{aligned} F^{+-}_{\rm QL} =& \Re\Pi^{--}\left[-G^{++}\,G^{+-} + G^{+-}\,G^{--}\right] \\ &+ i\Im\Pi^{--}\Big[G^{++}\,G^{+-} + G^{+-}\,G^{--} \\ &- \frac{2e^{\beta p_0}}{e^{\beta p_0}+1}\,G^{++}\,G^{--} - \frac{2}{e^{\beta p_0}+1} G^{+-}G^{+-}\Big], \end{aligned} \qquad \text{(D.4)}$$

where the arguments (X,k) are suppressed. Inserting the propagators of eq. (A.7) and using the fact that

$$G_{\rm F}(k) + G^*_{\rm F}(k) = -2\pi i\delta(k^2-m^2), \qquad \text{(D.5)}$$

one can express $F^{+-}_{\rm QL}$ in terms of $G_{\rm F}$ and $G^*_{\rm F}$. After some algebra one finds

$$\begin{aligned} F^{+-}_{\rm QL}(X,k) =& \Re\Pi^{--}(X,k)\left[G^2_{\rm F}(X,k) - G^{*2}_{\rm F}(X,k)\right] \\ &\times\left[\Theta(k_0) + n(|k|)\right] + i\Im\Pi^{--}(X,k) \\ &\times\left[G^2_{\rm F}(X,k) + G^{*2}_{\rm F}(X,k)\right]\frac{1}{e^{-\beta k_0}+1}. \end{aligned} \qquad \text{(D.6)}$$

No products of the form $G_{\rm F}\,G^*_{\rm F}$ occur, and therefore one may conclude that this expression is free of pinch singularities.

For the sum of the four rainbow graphs shown in fig. 6 R a) to R d), one obtains a similar expression by replacing the gluonic propagators by quark propagators and the self-energy insertion Π by the quark Fock self-energy $\Sigma_{F,q}$ shown in fig. 5. One finds

$$\begin{aligned} F^{+-}_{\rm R}(X,k) =& \Re\Sigma^{--}_{F,q}(X,k)\left[S^2_{\rm F}(X,k) - S^{*2}_{\rm F}(X,k)\right] \\ &\times\left[\Theta(k_0) + n(|k|)\right] + i\Im\Sigma^{--}_{F,q}(X,k) \\ &\times\left[S^2_{\rm F}(X,k) + S^{*2}_{\rm F}(X,k)\right]\frac{1}{e^{-\beta k_0}+1}, \end{aligned} \qquad \text{(D.7)}$$

which is also free of pinch singularities.

For the sum of the four ladder graphs shown in fig. 6 L a) to L d) one cannot perform an analogous calculation since the graph $\Sigma^{+-}_{\rm Ld)}$ vanishes due to the vertices with three on-shell gluons. One finds the expression for $F^{+-}_{\rm L}(X,k)$ to be

$$F^{+-}_{\rm L} = G^{++}\tilde{\Pi}^{+-}G^{--} + G^{++}\tilde{\Pi}^{++}G^{+-} + G^{+-}\tilde{\Pi}^{--}G^{--}, \qquad \text{(D.8)}$$

where $\tilde{\Pi}$ is the gluonic Fock self-energy $\Sigma^{-+}_{F,g(a)}$ shown in fig. 5a). Since pinch singularities can occur only on-shell, we consider now the self-energy insertions on-shell and find

$$\begin{aligned} \tilde{\Pi}^{+-}(X;E_k,\vec{k}) &= \tilde{\Pi}^{-+}(X;E_k,\vec{k}) \\ &= \Im\tilde{\Pi}^{--}(X;E_k,\vec{k}) = 0\,, \end{aligned} \qquad \text{(D.9)}$$

$$\begin{aligned} \tilde{\Pi}^{--}(X;E_k,\vec{k}) &= -\tilde{\Pi}^{++}(X;E_k,\vec{k}) \\ &= \Re\tilde{\Pi}^{--}(X;E_k,\vec{k}). \end{aligned} \qquad \text{(D.10)}$$

Inserting this into eq. (D.8) yields

$$\begin{aligned} F^{+-}_{\rm L}(X;E_k,\vec{k}) &= \Re\tilde{\Pi}^{--}(X;E_k,\vec{k}) \\ &\times\left[G^2_{\rm F}(X;E_k,\vec{k}) - G^{*2}_{\rm F}(X;E_k,\vec{k})\right]\left[\Theta(k^0) + n(|k|)\right]. \end{aligned} \qquad \text{(D.11)}$$

This expression is also free from pinching, and therefore $F^{+-}_L(X,k)$ for arbitrary k has no pinch singularities.

We summarize that in equilibrium in single two-loop self-energy graphs pinch singularities can occur, but the sum of the graphs a) to d) of one generic type (*i.e.* rainbow, ladder or quark-loop graphs) is free of pinching.

More examples of the cancellation of pinch singularities in equilibrium are given, *e.g.*, in [38].

References

1. F. Reif, *Fundamentals of Statistical and Thermal Physics* (McGraw-Hill Book Company Japan, Auckland, 1965).
2. J. Schwinger, J. Math. Phys. **2**, 407 (1961).
3. L.V. Keldysh, JETP **20**, 1018 (1965).
4. K. Geiger, B. Müller, Nucl. Phys. B **369**, 600 (1992).

5. K. Geiger, B. Müller, Phys. Rev. D **50**, 337 (1994).
6. K. Geiger, Phys. Rev. D **54**, 949 (1996).
7. S. Mrówczyński, U. Heinz, Ann. Phys. (N.Y.) **229**, 1 (1994).
8. D.S. Isert, S.P. Klevansky, hep-ph/9912203.
9. S.P. Klevansky, A. Ogura, J. Hüfner, Ann. Phys. (N.Y.) **261**, 37 (1997).
10. H. Umezawa, H. Matsumoto, M. Tachiki, *Thermo Field Dynamics and Condensed States* (North-Holland Publishing Company, Amsterdam, 1982).
11. K. Werner, Phys. Rep. **232**, 87 (1993).
12. H.-Th. Elze, M. Gyulassy, D. Vasak, H. Heinz, H. Stöcker, W. Greiner, Mod. Phys. Lett. A **2**, 451 (1987).
13. W. Cassing, S. Juchem, Nucl. Phys. A **665**, 377 (2000).
14. D.F. Litim, C. Manuel, Nucl. Phys. B **562**, 237 (1999).
15. J.-P. Blaizot, E. Iancu, Nucl. Phys. B **557**, 183 (1999).
16. J.C. Polkinghorne, J. Math. Phys. **4**, 503; 1393; 1396 (1963).
17. J.R. Forshaw, D.A. Ross, *Quantum Chromodynamics and the Pomeron* (Cambridge University Press, Cambridge, 1997).
18. W. Botermans, R. Malfliet, Phys. Rep. **198**, 115 (1990).
19. K.-C. Chou, Z.-B. Su, B.-L. Hao, L. Yu, Phys. Rep. **118**, 1 (1985).
20. L.D. Landau, E.M. Lifschitz, *Course of Theoretical Physics, Physical Kinetics*, Vol. **10** (Pergamon Press, Oxford, 1981).
21. L.P. Kadanoff, G. Baym, *Quantum Statistical Mechanics* (Benjamin, New York, 1962).
22. J.E. Davis, R.J. Perry, Phys. Rev. C **43**, 1893 (1991).
23. M. Le Bellac, *Thermal Field Theory* (Cambridge University Press, Cambridge, 1996).
24. R.L. Kobes, G.W. Semenoff, Nucl. Phys. B **260**, 714 (1985).
25. R.L. Kobes, G.W. Semenoff, Nucl. Phys. B **272**, 329 (1986).
26. P.F. Bedaque, A. Das, S. Naik, Mod. Phys. Lett. A **12**, 2481 (1997).
27. F. Gelis, Nucl. Phys. B **508**, 483 (1997).
28. R. Baier, M. Dirks, K. Redlich, Phys. Rev. D **55**, 4344 (1997).
29. N.P. Landsman, Ch.G. van Weert, Phys. Rep. **145**, 141 (1987).
30. H. Matsumoto, I. Ojima, H. Umezawa, Ann. Phys. (N.Y.) **152**, 348 (1984).
31. I. Dadić, Phys. Rev. D **59**, 125012 (1999).
32. C. Greiner, S. Leupold, Eur. Phys. J. C **8**, 517 (1999).
33. P.F. Bedaque, Phys. Lett. B **344**, 23 (1995).
34. T. Altherr, Phys. Lett. B **341**, 325 (1995).
35. Ch.G. van Weert, in *Proceedings of the Workshop on Thermal Field Theory, Banff, 1993*, edited by F.C. Khanna, R. Kobes, G. Kunstatter, H. Umezawa (World Scientific, Singapore, 1994).
36. M. van Eijck, *Thermal Field Theory and the Finite-Temperature Renormalization Group*, Thesis, University of Amsterdam (1995).
37. Yu.L. Dokshitzer, *Lecture Notes in Physics*, edited by F. Lenz, H. Grießhammer, D. Stoll, Vol. **496** (Springer, Berlin, Heidelberg, 1997).
38. Y. Fujimoto, R. Grigjanis, Z. Phys. C **28**, 395 (1985).